

Solutions for improving the energy efficiency in wastewater treatment plants based on solid oxide fuel cell technology

Original

Solutions for improving the energy efficiency in wastewater treatment plants based on solid oxide fuel cell technology / Gandiglio, M.; Saberi Mehr, A.; Mosayebnezhad, M.; Lanzini, A.; Santarelli, M.. - In: JOURNAL OF CLEANER PRODUCTION. - ISSN 0959-6526. - 247:(2020), p. 119080. [10.1016/j.jclepro.2019.119080]

Availability:

This version is available at: 11583/2779796 since: 2020-01-13T19:34:06Z

Publisher:

Elsevier Ltd

Published

DOI:10.1016/j.jclepro.2019.119080

Terms of use:

This article is made available under terms and conditions as specified in the corresponding bibliographic description in the repository

Publisher copyright

IEEE postprint/Author's Accepted Manuscript

©2020 IEEE. Personal use of this material is permitted. Permission from IEEE must be obtained for all other uses, in any current or future media, including reprinting/republishing this material for advertising or promotional purposes, creating new collecting works, for resale or lists, or reuse of any copyrighted component of this work in other works.

(Article begins on next page)

Solutions for improving the energy efficiency in wastewater treatment plants based on solid oxide fuel cell technology

Marta Gandiglio¹, Ali Saberi Mehr^{2,*}, Mohsen MosayebNezhad^{1,3}, Andrea Lanzini¹,
Massimo Santarelli^{1,4,5}

1. Department of Energy, Politecnico di Torino, Turin, Italy

2. Department of Mechanical Engineering, University of Bonab, Bonab, Iran

3. Faculty of Aerospace Engineering, Delft University of Technology, Delft, The Netherlands

4. Energiteknik, KTH, Stockholm, Sweden

5. Department of Mechanical and Industrial Engineering, University of Illinois at Chicago, Chicago, IL, United States

Abstract

Polygeneration configurations for small power generation systems offer significant potential for energy saving and reducing carbon emissions in wastewater treatment facilities. In this work, a biogas-fed solid oxide fuel cell system operating in a wastewater treatment plant (located in Turin, Italy) is analyzed in terms of its potential improvements through novel polygeneration systems. In its present combined heat and power configuration, along with electrical power, thermal energy from the exhaust gas is recovered to provide required heat to the plant's anaerobic digester. The analysis is focusing on different energy efficiency solutions for this type of plant by using solar thermal collectors, microturbines, a trilateral Rankine cycle, and an absorption chiller. Results reveal that, despite of higher efficiency for the trigeneration case using both trilateral Rankine cycle and absorption chiller (up to 88.4 %), the solar integrated system results in the lowest natural gas consumption, which is 38.5 % lower than the baseline scenario. This same scenario is also the worst in economic terms due to the high capital costs of solar collectors. In a short-term cost trajectory of the solid oxide fuel cell technology, the most economically favorable scenario is the microturbine integrated case in which the calculated levelized cost of electricity is 0.11 €/kWh, lower than grid electricity price, and with payback time of 6.5 years. Long-term cost trajectory is indeed generating effective investments for all of the four scenarios with payback time between 3 and 5 years in all cases. The analysis has been developed to the entire European Union area: the most suitable market conditions are found in Germany, Denmark, Slovakia, and Italy.

Keywords: *solid oxide fuel cell, solar thermal system, microturbine, trilateral Rankine cycle, biogas, economic analysis.*

*Corresponding author: Ali Saberi Mehr
Email address: A.S.Mehr@tabrizu.ac.ir (ali.saberi07@gmail.com)
Tel: (+98) 4137745000 -1620

38 **Highlights**

39

- 40 • Different polygeneration solutions for installation at WWTP are analyzed.
- 41 • Thermodynamic and techno-economic models are created for polygeneration systems.
- 42 • Integration of microturbines is the most economic solution with LCOE of 0.11
- 43 €/kWh.
- 44 • The techno-economic analysis is extended for the entire EU area.
- 45 • Suitable market conditions are found in Germany, Denmark, Slovakia, and Italy.

46 1. Introduction

47 Water is a natural asset, sometimes in scarce supply and fundamental to life on Earth. Just 3
48 % of the planet's water is freshwater, of which only one third is accessible for use in
49 agriculture and diurnal human consumption. The rest is frozen in glaciers or hidden too deep
50 underground. Nowadays, an enormous number of facilities are in service worldwide to make
51 wastewater recycled. Similar to any other facilities, wastewater treatment plants (WWTPs)
52 require a great amount of electrical and thermal energy in order to run the plant
53 uninterruptedly. As shown in Figure 1, a typical wastewater treatment plant involves
54 processes listed below (MosayebNezhad et al., 2019) :

- 55 • In the first stage, wastewater is transferred to the plant by gravity through the central
56 sewer system. One could observe a variety of objects with different sizes and
57 elements reaching the WWTPs.
- 58 • In the preliminary treatment or pre-treatment which is the first mechanical stage, in
59 order to settle out the sand and grit, water flows through the gravel chamber. Then,
60 gravel is disposed of. Further, the bar screens are used to remove large substances
61 from the wastewater. Firstly, the coarse screens are implemented and then the fine
62 screens are used to remove smaller elements such as plastic films and cigarette butts.
- 63 • Grit is supposed to be separated from the wastewater next to the removal of large
64 objects. Like the gravel chamber, grit chamber allows the settlement of grit.
65 Afterward, grit is taken out of the tank and disposed of at the dump. Due to the high
66 contamination levels of both gravel and grit, neither of them can be reused.
- 67 • In the primary treatment known as “pre-settling basins”, water is guided to the hopper
68 in the tank base. At the velocity of about 4 cm/s, the hopper arm moves around the
69 edge of the tank. Treated water is steered towards edges and higher sedimentation
70 velocity than flowing fluid leads to settlement of particulates on the tank bottom. Here
71 the primary pre-treatment finishes and secondary wastewater treatment begins. At the
72 end of the primary treatment, the level of wastewater pollution cuts down to about 60
73 %.
- 74 • The biological stage which is the secondary treatment, is based on natural processes.
75 WWTPs use bacteria digesting the contaminants including biodegradable organics,
76 phosphorus and carbon. Subsequently, dead bacteria and organic residues convert to
77 sludge.

- 78 • During the secondary treatment, the excess sludge is moved before the settling tanks
79 by pumping it out. This is the point where the sludge settles and is guided to digestion
80 tanks for next level of treatment.
- 81 • Sludge which is pumped out of the digestion tanks is then heated and mixed. During
82 the digestion process, biogas is produced from the sludge. WWTPs can reuse the
83 biogas for electrical and thermal energy production.
- 84 • The second digestion stage happens in storage tanks when sludge digestion comes at
85 its optimal level. The water is separated from the semi-solid sludge, and sent back for
86 next treatment while the residual semi-solid experiences mechanical dewatering.
- 87 • Finally, sludge and dewatered to the optimal degree are disposed of at the
88 dump. About a month should pass so that the sludge is suitably dried out. However, it
89 can be complied with agricultural standards to be utilized as fertilizer for industrial
90 crops.
- 91 • The final step of wastewater treatment is the profound inspection of service
92 water. The main purpose is to evaluate the contamination level and ensure that the
93 highest standards are achieved.

94 Depending on the wastewater treatment plant, the electrical and thermal demand would be
95 different. Accordingly, depending on the size of the WWTP and the person equivalent served
96 the electrical demand of the WWTPs usually is in the range of 300kW to 1000kW which
97 could be suitable for medium size movers (Guerrini et al., 2017; Wellinger et al., 2013).
98 Considering the steps discussed above, there is a possible solution to supply the demand by
99 means of the utilization of biogas produced in the plant itself. Utilization of biogas produced
100 in the plant in order to supply the demand of the wastewater treatment plants has been
101 investigated in the literature. Conventionally, the produced biogas was burnt in a boiler to
102 supply only the thermal demand of the plant, a part of which were thermal demand of the
103 digester itself. To produce electricity, some plants have used an internal combustion engine
104 (ICE) or micro gas turbine (MGT) to utilize the biogas. In literature, other more sophisticated
105 solutions are analyzed. For a target biogas plant in Busan, Republic of Korea,
106 thermoeconomics of a biogas-fueled micro gas turbine (MGT) system combining with a
107 bottoming organic Rankine cycle (ORC), is performed by Sung et al. (Sung et al., 2017). It is
108 reported that where natural gas prices are high and electricity prices are low (such as in
109 Korea), the competitiveness of selling directly the biogas is very high compared to a power
110 generation system. The optimum size of MGT cogeneration in a sewage treatment plant in

111 terms of its economic performance is analyzed by Basrawi et al. (Basrawi et al., 2017). One
112 of the main results of their work is that the net present value could be obtained when the input
113 fuel of MGT is equal to the biogas production of the sewage treatment plant. On the other
114 hand, in the cases of heat demand fluctuation throughout the year, the smaller size of MGT
115 would be preferable.

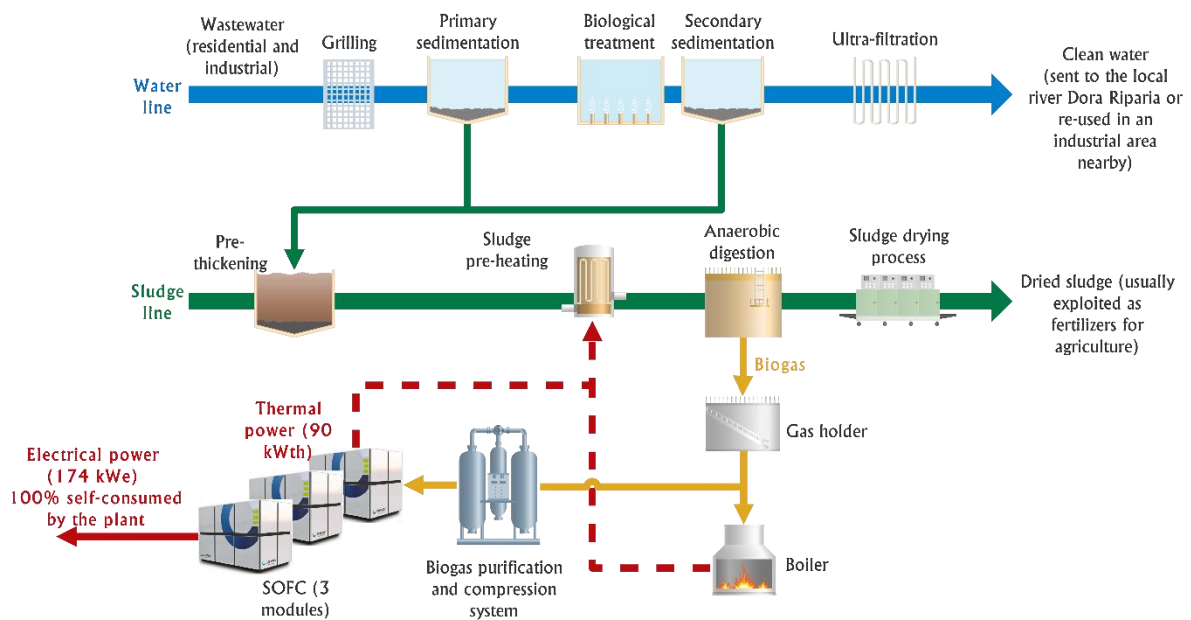
116 One of the promising technologies in producing power is Fuel Cell technology. Among
117 different types of fuel cell systems, Solid oxide fuel cell (SOFC) is an interesting choice as it
118 is modular, scalable, and more efficient. Compared to other fuel cells, the SOFCs are fuel-
119 flexible and can reform methane internally, use even carbon monoxide as a possible fuel, and
120 tolerate some degree of common fossil fuel impurities, such as ammonia and chlorides (Cui
121 et al., 2014). The energy analysis of two CHP plants using internal combustion engines (ICE)
122 and SOFC systems by feeding biogas is investigated by Santarelli et al. (Santarelli et al.,
123 2012). The comparison showed that the CHP plant based on SOFC system would be better
124 from the thermodynamics point of view. However, it is shown that the produced thermal
125 energy is quite higher for the case of ICE. Williams et al. (Williams et al., 2001) proposed an
126 indirect SOFC-GT hybrid system. They reported that the maximum achievable efficiency for
127 their system is 45 %. In addition, it is shown that the system has lower efficiency value than
128 that of the direct combination of the two systems. Cheddie et al. (Cheddie and Murray,
129 2010a) evaluated a combined system including an SOFC system and a 10 MW gas turbine
130 plant. Considering to the developed thermo-economic model, it is reported that the proposed
131 system could generate 20.6 MW power at the electrical efficiency of 49.9 %. In their
132 following research (Cheddie and Murray, 2010b), an integration of SOFC and gas turbine in a
133 semi-integrated configuration was investigated. It is revealed that an output power of 21.6
134 MW could be generated at the efficiency of 49.2 %. A new model for evaluation an SOFC-
135 GT system is proposed by Zhang et al. (Zhang et al., 2014) where the SOFC stack and the
136 combustion chamber exhaust gases are utilized to heat up the gas turbine inlet stream. Bicer
137 and Dincer (Bicer and Dincer, 2015) introduced a scheme including underground coal
138 gasification, steam-assisted gravity drainage, solid oxide fuel cell, integrated gasification
139 combined cycle and an electrolyzer. Energy and exergy efficiencies of 19.6 % and 17.3 % are
140 obtained for the combined system, respectively. Zhao et al. (Yan et al., 2013) investigated a
141 coal syngas-fueled SOFC stack working in an atmospheric condition integrated indirectly
142 with a Brayton cycle. The authors concluded that the system efficiency increases with
143 decreasing current density and the value could be in a range of 48-56 %, depending on the
144 operating temperature and current density. Inui et al. (Inui et al., 2005) proposed two
145 configurations of carbon dioxide recovering systems using the integration of SOFC-GT. It is

146 reported that applying the positive influence of the carbon dioxide recycle, the overall
147 efficiency of 70.88 % (based on LHV) could be obtained. These values for the system with
148 water vapor injection are 65.00 % (HHV) or 72.13 % (LHV), respectively. Eveloy et al.
149 (Eveloy et al., 2016) investigated an indirect combination of an SOFC system and a gas
150 turbine with an organic Rankine cycle. It is stated that the SOFC-GT-ORC system
151 demonstrates an efficiency improvement of about 34 % compared to the gas turbine as a
152 stand-alone system, and of 6 % compared to the hybrid SOFC-GT sub-system. It is stated that
153 within three to six years depends on the working condition the profitability of the system is
154 varying. Inui et al. (Inui et al., 2003) suggested a system combining of an SOFC and a
155 magnetohydrodynamic (MHD)/noble gas turbine with a unit of carbon dioxide recovery. It is
156 reported that the overall thermal efficiency of the system using methane as the fuel could be
157 63.66 % (HHV) or 70.64 % (LHV) (Safari et al., 2016). At full and part loads, performance
158 of direct or indirect combination of SOFC and GT systems is analyzed and compared with
159 the performance of regenerative gas turbine by Sánchez et al. (Sánchez et al., 2008). It is
160 found that the direct hybrid system is superior to the indirect one as power and efficiency
161 enhancements because of the higher pressure in the SOFC are not accessible in the indirect
162 case. Results show that initial investment/installation cost of an integrated system is high in
163 spite of low total cost of a fuel-cell-based configuration. A new approach to combine
164 electrodeionization (EDI) and solid oxide fuel cells (SOFCs) is proposed by Xu et al. (Xu et
165 al., 2017). This system is integrated with anaerobic digestion/landfills to capture energy from
166 carbonaceous and nitrogenous pollutants. It is reported that under the optimal conditions, the
167 system obtained a higher net energy output compared to the conventional systems. The effect
168 of feeding SOFCs with biogas coming from anaerobic digestion is investigated by Lackey et
169 al. (Lackey et al., 2017). It is demonstrated that a great reduction in greenhouse gas emissions
170 could be achieved. Also, it is shown that higher humidification provides better performance
171 as the water gas shifting reaction produced more H₂ with additional H₂O.

172 In 2015, a European project namely DEMOSOFC, considering SOFC power systems for a
173 real wastewater treatment plant near Turin, Italy was proposed. The DEMOSOFC plant as
174 shown in Figure 1 comprises the following systems (“DEMOSOFC project official website,”
175 2018):

- 176 1. In the first stage, the biogas processing unit comprising biogas dehumidification,
177 disposing of contaminants, and compression is implemented. Biogas contains
178 siloxanes and hydrogen sulfide both of which are detrimental for the fuel cell
179 performance. An adsorption-based system using impregnated activated carbons is

- 180 considered for disposing of these contaminants. To this end, biogas should be cooled
 181 beforehand in order to ensure the carbon optimal operating parameters. At the inlet
 182 and outlet of the clean-up system, an online gas analyzer to detect both siloxanes and
 183 H₂S is set.
- 184 2. The electricity producing unit is composed of three SOFC modules, which generate
 185 about 58 kW_e per each unit.
- 186 3. Proposing a new heat recovery unit is to utilize the hot exhaust from the SOFC
 187 modules while a conventional water loop that is heated up by an existing boiler is
 188 being used in the plant.
- 189 4. To control the plant from both on-site and remotely a supervisory, control and data
 190 acquisition (SCADA) system is used.



191
 192 Figure 1. Concept diagram of the DEMOSOFC plant (“DEMOSOFC project official website,” 2018).

193 Currently, the project is in the final phase and SOFC units are being deployed in the plant as
 194 shown in Figure 2.



195

196 Figure 2. The DEMOSOFC plant after commissioning of the second SOFC unit (“SMAT, Società Metropolitana
197 Acque Torino S.p.A., Turin, IT.,” 2019).

198 Previously, supplying the electrical and thermal demands of WWTPs by means of ICE
199 (Santarelli et al., 2012), MGT (MosayebNezhad et al., 2018) and SOFC (Mehr et al., 2017)
200 were investigated in several works. However, a comprehensively comparative study revealing
201 which configuration could be promising was carried out. In addition, most of the systems
202 presented before did not consider the process of digester thermal load which plays a central
203 role in producing biogas in the plant.

204 In the present work, four different scenarios, using SOFC unit as the primary electric power
205 generator, and evolving to a poly-generative configuration are proposed. A comprehensive
206 thermo-economic analysis is performed, and the performance of the proposed systems is
207 compared with each other. In order to provide a meaningful comparison, the DEMOSOFC
208 project is considered as the base case so that the proposed scenarios can be compared with a
209 real life ongoing project. Finally, based on the results, the best possible solution from the
210 energetic and techno-economic points of view for the WWTP is explained.

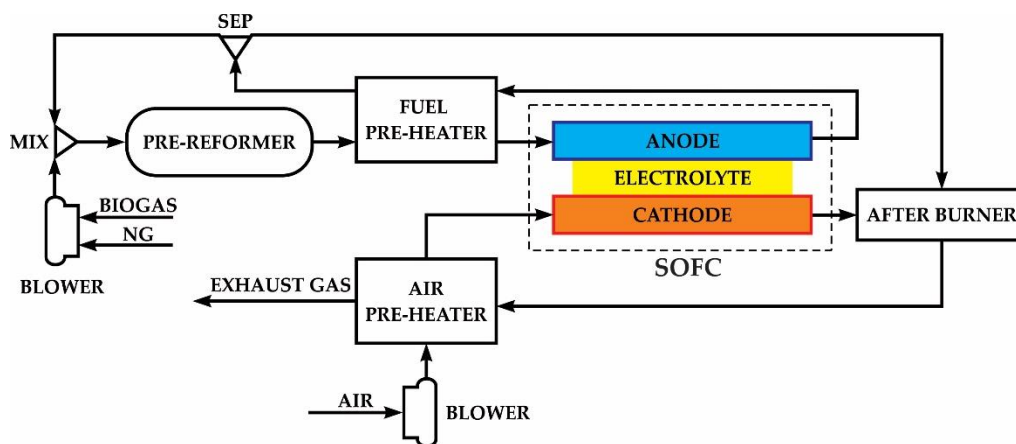
211 **2. Description of the systems**

212 In this section different configurations of the proposed and investigated systems are
213 explained.

214 **1.1 SOFC system**

215 Figure 3 demonstrates the SOFC system configuration which has been analyzed in the
216 present study. A mixture of the natural gas from the grid and biogas produced in the

217 wastewater treatment plant is the fuel which is sent to the anode of the SOFC unit in order to
 218 produce electricity. The mixture is first sent to the pre-reformer before which the fuel is
 219 mixed with high temperature anode recycle gases. Through reforming and shifting reactions
 220 in the pre-reformer, complex and heavy chains of hydrocarbons are cracked, and a fraction of
 221 fuel (CH_4) is transferred into carbon monoxide and hydrogen. In order to obtain a determined
 222 fuel temperature before sending it to the anode for the electrochemical reaction, the fuel is
 223 heated through the fuel heat exchanger. As it can be observed, anode recycle gases are used
 224 to heat up the fuel. A suitable separator is equipped to divide the anode recycle gases into two
 225 streams. A part of gases is sent to the mixing unit while the rest is utilized in the after-burner.
 226 On the other side, the air is preheated through an air heat exchanger by receiving the thermal
 227 energy from the after-burner exhaust gases. Notice that, two blowers are used to increase the
 228 pressure of the fuel and air before sending them into the system. The blowers are just
 229 equipped in order to compensate the pressure drops within the system and not to increase the
 230 pressure of the SOFC system. So the SOFC system is operated at nearly the atmospheric
 231 pressure.



232
 233 Figure 3. Proposed SOFC system layout.

234 1.2 Scenarios

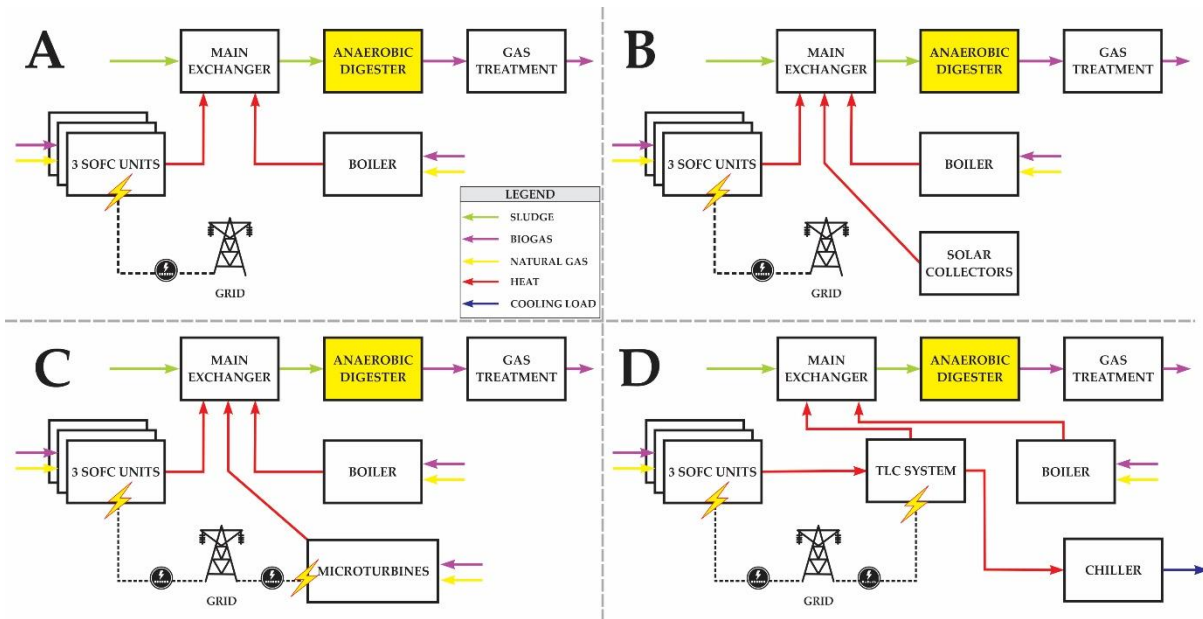
235 There is a notable potential of the available biogas in the SMAT Collegno for electricity
 236 generation. Considering the SOFC units to generate power as a base scenario, which was
 237 supposed to be realized in DEMOSOFC project, base case layout is defined. Here, to provide
 238 the digester heat the available biogas from the plant is just to be fed to the SOFC units.

239 In the second scenario, solar collectors are used in parallel to the boiler in order to supply a
 240 part of the thermal load of the digester.

241 As an upgraded layout, the MGT case including a new integration of SOFC and micro gas
 242 turbines in the WWTP is introduced as the third scenario. In this case, a micro gas turbine is

243 used to compensate a part of digester thermal energy demand. In addition, the whole system
 244 could produce extra electricity.

245 The last scenario which is called Trigen case is defined as a combined cooling and heating
 246 power (CCHP) system integrating SOFC units with trilateral Rankine cycle (TLC) system
 247 and an absorption chiller. The exhaust gas from SOFC systems is first sent to the TLC
 248 evaporator to run the system, and then the gases are utilized in an absorption chiller to
 249 produce cooling effects. In this case, the thermal demand of digester will be supplied by both
 250 the TLC condenser and the main boiler.



251
 252 Figure 4. Proposed configurations: A) Base case, B) Solar case, C) MGT case, and D) Trigen case.

253 The detailed energy modeling of the proposed systems in the previous section has been
 254 performed in the authors' works (Gandiglio et al., 2016; Mehr et al., 2018, 2017; Yari et al.,
 255 2016). However, comparative techno-economic analysis for all proposed systems,
 256 particularly the Trigen case, has not been carried out yet. Therefore, in the present work, it is
 257 tried to provide full economic investigation, as well as extending the economic analysis for
 258 the entire EU area.

259 2. Energetic investigation

260 The energy modeling of the proposed systems is described in this section in detail.

261 2.1 Assumptions

262 Some meaningful assumptions were used in the present simulation:

- 263 • Air is considered to contain 79 % N₂ and 21 % O₂ neglecting other tiny components.

- 264 • Gas leakage from the components and pipelines is neglected.
- 265 • Cathode and anode temperatures are assumed to be identical.
- 266 • Accordingly (Gandiglio et al., 2016), the available biogas in the plant containing 65%
- 267 CH₄ and 35 % CO₂ on a volume basis.
- 268 • The priority is to utilize the available biogas produced in the plant as much as
- 269 possible.
- 270 • The type of digester is mesophilic.

271 2.2 Solid oxide fuel cell modeling

272 By means of an electrochemical process occurred in SOFC stack, DC power can be produced.
 273 The fuel (biogas) containing methane gas is reformed inside the anode side in order to finally
 274 produce H₂ which is oxidized in the SOFC. DC power is produced as;

$$\dot{W}_{FC,stack} = N_{FC} \cdot j \cdot A_a \cdot V_c \quad (1)$$

275 Where NFC is the number of the cells, j is the current density, A_a is the active area of cells
 276 and V_c is the actual cell voltage. The key point in calculating the SOFC power is to
 277 determine the actual cell voltage. It is defined as:

$$V_c = V_N - V_{loss} \quad (2)$$

278 Here, V_N is the Nernst voltage expressing as;

$$V_N = -\frac{\Delta \bar{g}^o}{2F} + \frac{\bar{R}T_{FC,e}}{2F} \ln \left(\frac{a_{H_2}^{Anode,exit} \sqrt{a_{O_2}^{Cathode,exit}}}{a_{H_2O}^{Anode,exit}} \right) \quad (3)$$

279 V_{loss} the voltage loss, which is the sum of ohmic, activation and concentration voltage losses:

$$V_{loss} = V_{ohm} + V_{act} + V_{conc} \quad (4)$$

280 Ohmic loss is formulated as (See also

281 Table 1):

$$V_{ohm} = (R_{int} + \rho_{an}L_{an} + \rho_{cat}L_{cat} + \rho_{ely}L_{ely}) j \quad (5)$$

282

283 Table 1. Material features for estimating the Ohmic voltage loss (Wongchanapai et al., 2012).

Component	Material type	Thickness (mm)	Resistivity
Anode	Ni/YSZ cermet	0.5	$\rho_{an}=2.98 \times 10^{-5} \exp\left(\frac{-1392}{T_{FC,e}}\right)$
Electrolyte	YSZ	0.01	$\rho_{ely}=2.94 \times 10^{-5} \exp\left(\frac{10350}{T_{FC,e}}\right)$
Cathode	LSM-YSZ	0.05	$\rho_{cat}=8.114 \exp\left(\frac{600}{T_{FC,e}}\right)$
Interconnection	Doped LaCrO ₃	-	0.0003215

284

285 The activation voltage loss is the sum of losses for both the anode and cathode sides;

$$V_{act} = V_{act,a} + V_{act,c} \quad (6)$$

$$V_{act,a} = \frac{\bar{R}T_{FC,e}}{F} (\sinh^{-1}(\frac{j}{2j_{oa}})) \quad (7)$$

$$V_{act,c} = \frac{\bar{R}T_{FC,e}}{F} (\sinh^{-1}(\frac{j}{2j_{oc}})) \quad (8)$$

286 Where j_o is the exchange current density and it can be calculated for the anode and cathode

287 sides using the following equations;

$$j_{0,a} = \gamma_{an} \left(\frac{RT}{2F}\right) e^{\left(\frac{-E_{a,an}}{RT}\right)} \quad (9)$$

$$j_{0,c} = \gamma_{cat} \left(\frac{RT}{2F}\right) e^{\left(\frac{-E_{a,cat}}{RT}\right)} \quad (10)$$

288 Notice that pre-exponential and active energy values for anode are 6.54×10^{11} A/m² and 140289 kJ/mol while these parameters for the cathode are 2.35×10^{11} A/m² and 137 kJ/mol

290 (Wongchanapai et al., 2012; Yari et al., 2016). Anode electrochemical semi-reaction results

291 in the hydrogen consumption at the electrode-electrolyte interface. Since the fresh fuel could

292 not readily replace the hydrogen, its partial pressure drops resulting in a reduction of the cell

293 voltage. Meanwhile, a similar phenomenon happens at the cathode compartment where

294 oxygen is consumed in the cathode electrode. This overvoltage can be calculated taking into

295 account transportation phenomena occurring in the fuel cell. It is usually negligible for low

296 current density while for high current densities it becomes a major issue in producing power
 297 by the fuel cell. Concentration is usually simulated neglecting heat convection and taking
 298 into account only diffusion phenomena, introducing binary and Knudsen diffusion models.

299 Concentration loss is also can be expressed as;

$$V_{conc} = V_{conc,a} + V_{conc,c} \quad (11)$$

300 where

$$V_{conc,an} = \frac{RT}{2F} \ln\left(\frac{P_{H_2} \times P_{H_2O,TPB}}{P_{H_2O} \times P_{H_2,TPB}}\right) \quad (12)$$

301 And

$$V_{conc,cat} = \frac{RT}{4F} \log\left(\frac{P_{O_2}}{P_{O_2,TPB}}\right) \quad (13)$$

302 where the subscript TPB denotes the three-phase boundary. To calculate the pressure at the
 303 reaction sites, the following equations are used:

$$P_{H_2O,TPB} = P_{H_2O,an} + j \frac{R T_{FC} L_{an}}{2 F D_{an,H_2}^{eff}} \quad (14)$$

$$P_{H_2,TPB} = P_{H_2,an} - j \frac{R T_{FC} L_{an}}{2 F D_{an,H_2O}^{eff}} \quad (15)$$

$$P_{O_2,TPB} = P_{cat} - (P_{cat} - P_{O_2,cat}) \exp\left(j \frac{R T_{FC} L_{cat}}{4 F D_{O_2}^{eff} P_{cat}}\right) \quad (16)$$

307 where, $D_{H_2}^{eff}$, $D_{H_2O}^{eff}$ and $D_{O_2}^{eff}$ are the effective gaseous diffusivity through the anode (for H2),
 308 anode (for H₂O) and the cathode (for O₂), respectively. The effective gaseous diffusivity can
 309 be calculated as:

$$\frac{1}{D_{an,H_2}^{eff}} = \frac{\epsilon_{an}}{\tau_{an}} \left(\frac{1}{D_{H_2,K}} + \frac{1}{D_{H_2,H_2O}} \right) \quad (17)$$

$$311 \quad \frac{1}{D_{an,H_2O}^{eff}} = \frac{\varepsilon_{an}}{\tau_{an}} \left(\frac{1}{D_{H_2O,K}} + \frac{1}{D_{H_2O,H_2}} \right) \quad (18)$$

$$312 \quad \frac{1}{D_{cat,O_2}^{eff}} = \frac{\varepsilon_{cat}}{\tau_{cat}} \left(\frac{1}{D_{O_2,K}} + \frac{1}{D_{O_2,N_2}} \right) \quad (19)$$

313 Where the porosity (ε) and tortuosity (τ) of electrode materials are estimated to be 0.48
 314 and 5.4, respectively. To calculate the effective gaseous diffusivity, combined ordinary and
 315 Knudsen diffusion should be defined and calculated using the following equations;

$$316 \quad D_{H_2,K} = 97 r_{pore,an} \sqrt{\frac{T_{FC}}{M_{H_2}}} \quad (20)$$

$$317 \quad D_{H_2O,K} = 97 r_{pore,an} \sqrt{\frac{T_{FC}}{M_{H_2O}}} \quad (21)$$

$$318 \quad D_{O_2,K} = 97 r_{pore,cat} \sqrt{\frac{T_{FC}}{M_{O_2}}} \quad (22)$$

$$319 \quad D_{H_2,H_2O} = \frac{1.43 \times 10^{-7} T_{FC}^{1.75}}{\sqrt{M_{H_2,H_2O}} (V_{H_2}^{1/3} + V_{H_2O}^{1/3})^2 P} \quad (23)$$

$$320 \quad D_{O_2,N_2} = \frac{1.43 \times 10^{-7} T_{FC}^{1.75}}{\sqrt{M_{O_2,N_2}} (V_{O_2}^{1/3} + V_{N_2}^{1/3})^2 P} \quad (24)$$

321 Where M is the molecular weight of species, V represents diffusion volume of species.

322 Meanwhile, pore radius value (rpore) is estimated to be $0.5 \mu m$.

323 **2.3 Thermal and electrical demand of the WWTP**

324 For the comparison purpose, the real wastewater treatment plant in Torino, Italy is considered
 325 in this study as a reference plant (the SMAT Collegno WWTP, site of the DEMOSOFC
 326 plant). For the considered plant, thermal and electrical demand are shown in Figure 5. As it
 327 can be observed, the average electrical power and thermal power required in the plant is
 328 about 720 kW and 280 kW respectively. Notice that the electrical demand is provided by
 329 onsite measurements at the SMAT site, while the thermal load needed for maintaining the

330 digester temperature in a suitable range is calculated according to the digester design
 331 procedure, as follows.

332 On a monthly basis, the digester thermal load ($\dot{Q}_{digester}$) is calculated as the sum of the
 333 following terms:

- 334 • the thermal power required for the sludge heating up: from a variable inlet temperature
 335 (14-23°C depending on the season) to the digester temperature (38-47°C, taken from real
 336 hourly WWTP measurements), \dot{Q}_{sludge}
- 337 • \dot{Q}_{loss} which is accounted as for the heat losses through the digester walls;

$$\dot{Q}_{digester} = \dot{Q}_{sludge} + \dot{Q}_{loss} \quad (25)$$

338 The first term in (Eq. 14) is calculated assuming the followings:

- 339 • The sludge mass flow rate \dot{m}_{sludge} (the average monthly value is used as calculated from
 340 the SMAT hourly measurements)
- 341 • The sludge inlet temperature $T_{sludge,in}$ (Mazzini, 2014; Pizza, 2015)
- 342 • The digester constant temperature $T_{digester}$
- 343 • The specific heat capacity c_p is the same as to that of water because the solid content in
 344 sludge is lower than 2 % (weight).

345 The sludge pre-heating term is calculated as:

$$\dot{Q}_{sludge} = \dot{m}_{sludge} \cdot c_p \cdot (T_{digester} - T_{sludge,in}) \quad (26)$$

346 The heat losses can be expressed as;

$$\dot{Q}_{loss} = \dot{Q}_{underground} + \dot{Q}_{external} + \dot{Q}_{piping} \quad (27)$$

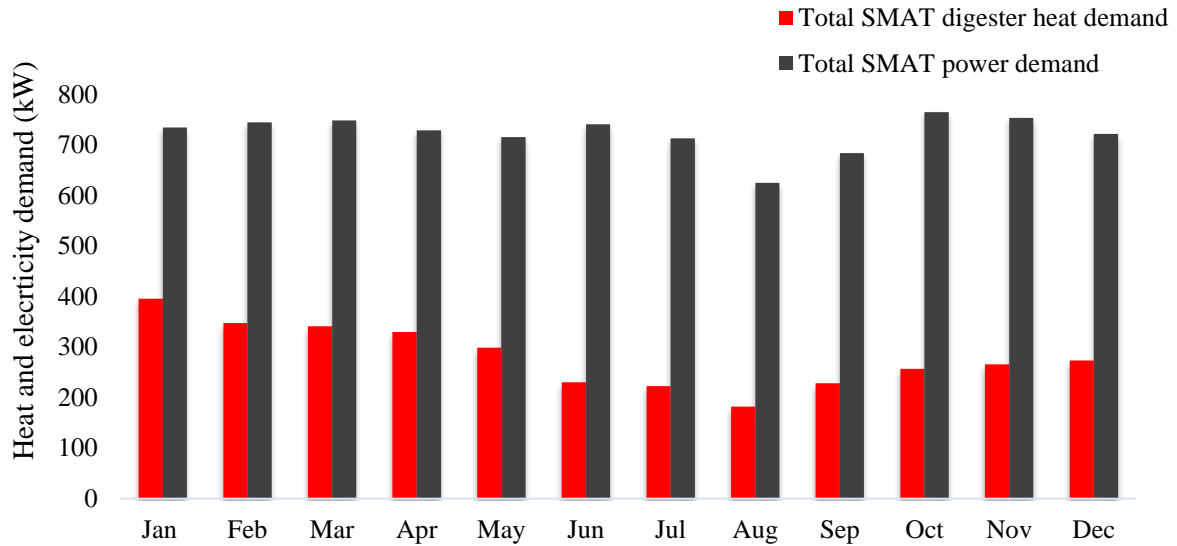
347 Where:

$$\dot{Q}_{underground} = U_{underground} \cdot A_{underground} \cdot (T_{digester} - T_{ground}) \quad (28)$$

$$\dot{Q}_{external} = U_{external} \cdot A_{external} \cdot (T_{digester} - T_{external}) \quad (29)$$

$$\dot{Q}_{pipes} = 0.05 \cdot (\dot{Q}_{sludge} + \dot{Q}_{underground} + \dot{Q}_{external}) \quad (30)$$

348 $\dot{Q}_{underground}$ is the contribution for heat losses from the underground surface and $\dot{Q}_{external}$
 349 accounts for heat losses through the external surface (walls and roof). The calculated values
 350 of thermal energy for digester is illustrated in Figure 5. As the figure indicates, the needed
 351 thermal and electrical demands in summer are less than those in other seasons because of the
 352 lower wastewater inflow during the summer time.



353

354 Figure 5. Required thermal energy for digester and electrical demand in SMAT Collegno reported for 2015.

355 Table 2. Factors for calculations of digester thermal load (all data are retrieved from the SMAT Collegno
 356 anaerobic digester sizing report, (FISIA, 2018).

Parameter	Unit	Value
for underground walls $U_{underground}$	W/m ² °C	2.326
for non-underground walls $U_{external}$	W/m ² °C	0.930
floor and partial side walls $A_{underground}$	m ²	450.8
partial side walls and roof $A_{external}$	m ²	1132.1

357

358 As discussed before, for each scenario the coverage of the thermal load would be different.
 359 For the base case, the boiler and the heat recovery from the SOFC exhaust gases would
 360 supply the digester thermal load. However, for the solar case, in addition to the boiler and
 361 SOFC systems, a parabolic solar system will be responsible for supplying the thermal
 362 demand. For the MGT case, the exhaust gas from MGT could partially supply the thermal
 363 energy. Supplying the thermal demand in the trigeneration case is somehow different. In this
 364 case, the SOFC exhaust gases will be utilized in TLC and absorption chiller, and the thermal
 365 demand of digester will be recovered by using the boiler and heat recovery system of TLC.

366 2.4 Proposed integrated systems

367 2.4.1 Solar Case

368 Parabolic trough collectors are located in the plant to receive the solar energy. It is basically
369 composed of a parabolic-trough-shaped concentrator which reflects direct solar radiation onto
370 a receiver or absorber tube located in the focal line of the parabola. The Parabolic Trough
371 Collectors (PTC) efficiency is not fix and depends on the heat losses as well as on the useful
372 heat carried by working fluid. The heat losses at air side are varied by environmental
373 temperature, cover temperature, and wind velocity.

374 The temperature difference between working fluid and surface determines the useful heat at
375 the working fluid side. To decrease the heat losses, an evacuated concentric glass tube is
376 employed around the receiver. The collector *IND300*, one of the smaller models of PTC
377 family is chosen. The IND 300 PTC's efficiency is reported as;

$$\eta_{IND300} = 0.733 - 0.238 \cdot \left(\frac{\bar{T}_{wf} - \bar{T}_0}{G} \right) - 0.0013 \left(\frac{\bar{T}_{wf} - \bar{T}_0}{G} \right)^2 \quad (31)$$

378 Where, \bar{T}_{wf} and G are the average collector working fluid temperature and direct (or beam)
379 normal irradiance (BNI), respectively, and \bar{T}_0 is the ambient temperature. The beam and
380 diffuse irradiances for the Turin city are available in ("National Renewable Energy
381 Laboratory (NREL). System advisor model (SAM).," 2018) on a monthly basis

382 2.4.2 MGT Case

383 The MGT system fed by biogas and natural gas is modeled though using each component of
384 the system as a control volume and applying the mass balance, and energy balance equations.

385 Some meaningful parameters at ISO conditions are considered for MGT system and listed in
386 Table 3.

387 Table 3. Parameters used for the components of the MGT system.

Parameter	Unit	Value
Turbine inlet temperature	°C	951
Exhaust temperature	°C	290
Compression ratio (CR)	-	4.6
Turbine isentropic efficiency (η_{GT})	%	85
Compressor isentropic efficiency (η_C)	%	85
Combustion efficiency (η_{CC})	%	99
Mechanical efficiency (η_M)	%	95
Generator efficiency (η_{EL})	%	94

Regeneration effectiveness (ϵ_{REG})	%	80
---	---	----

388

389 In this project, two commercially available microturbines (C30 and C65) from Capstone
390 Turbines Corporation are chosen since their thermal heat recovery potentials could bring the
391 required digester thermal demand (“Capstone Microturbine Products,” 2017). As for some
392 months there is a need to operate the MGT systems in partial load (PL), the partial load
393 analysis is also formulated as in Ref. (Firdaus et al., 2012).

$$\dot{W}_{MGT-30,PL} = \dot{W}_{MGT-30,FL} \times PL \quad (32)$$

$$\dot{Q}_{ehr,PL_{MGT-30}} = (0.1718 + 0.6529PL + 0.1706PL^2) \dot{Q}_{ehr,FL_{MGT-30}} \quad (33)$$

$$\dot{Q}_{fuel,PL_{MGT-30}} = (0.1513 + 0.7824PL + 0.06004PL^2) \dot{Q}_{fuel,FL_{MGT-30}} \quad (34)$$

$$\dot{W}_{MGT-65,PL} = \dot{W}_{MGT-65,FL} \times PL \quad (35)$$

$$\dot{Q}_{ehr,PL_{MGT-65}} = (0.1240 + 0.9707PL - 0.1706PL^2) \dot{Q}_{ehr,FL_{MGT-65}} \quad (36)$$

$$\dot{Q}_{fuel,PL_{MGT-65}} = (0.1228 + 0.9766PL - 0.1131PL^2) \dot{Q}_{fuel,FL_{MGT-65}} \quad (37)$$

394 It has been reported in the authors' previous research, implementing one C65 unit with one
395 C30 unit will be suitable for the plant (MosayebNezhad et al., 2018).

396 2.4.3 Trigeneration Case

397 Trilateral Rankine cycle generates the electrical power via its two-phase expander for which a
398 reasonable isentropic efficiency of 75 % (Yari et al., 2015) could be assumed.

$$\eta_{\text{expander}} = \frac{\dot{W}_{a, \text{expander}}}{\dot{W}_{s, \text{expander}}} \quad (38)$$

399 The modeling of the single effect LiBr-H₂O absorption refrigeration is based on the authors'
400 previous work (Yari et al., 2013).

401 2.5 Energy efficiency

402 One can define the overall energy efficiency for the plant as:

$$\eta_I = \frac{\sum \dot{W}_{produced} - \sum \dot{W}_{consumed} + \dot{Q}_{heating} + \dot{Q}_{cooling}}{\dot{m}_{biogas} \cdot LHV_{biogas} + \dot{m}_{NG} \cdot LHV_{NG}} \quad (39)$$

403 Where $\dot{W}_{produced}$ is the electrical power produced in the system by means of SOFC and/or
 404 MGT and/or TLC's expander. $\dot{W}_{consumed}$ is the electrical power consumed in the pumps
 405 and/or compressors and/or blowers. $\dot{Q}_{heating}$ is the total heat recovered in the system and
 406 $\dot{Q}_{cooling}$ is only defined for the trigeneration case where it is equipped with an absorption
 407 chiller. In the denominator, overall consumption of NG and biogas is given.

408 **2.6 Economic evaluation**

409 Starting from the results of the energy analysis, an economic evaluation of the investment has
 410 been performed for the four analyzed scenarios.

411 **2.6.1 Input data and cost functions**

412 Input data from the energy to the economic model are:

- 413 - Natural Gas (NG) consumption of the plant, used for the boiler feeding (for supplying
 414 heat when biogas from CHP is not enough).
- 415 - Electrical energy production from the available electrical generators depending on the
 416 scenarios (SOFC, MGT and TLC system)
- 417 - Heating and cooling energy production, where heat production is available only in the
 418 CHP case studies (solar, MGT and Trigen) and cooling only in the Trigen one.

419 Economic analysis has been calculated by evaluating investment costs spent during the year
 420 of construction (Capital Expenditure, CAPEX), operating costs required to run the plant on a
 421 yearly basis (Operating Expenditure, OPEX) and savings generated from the self-
 422 consumption of electricity, heating and cooling.

423 The CAPEX cost item is including:

- 424 - The cost of the Anaerobic Digester (AD), which is kept constant among the 4
 425 scenarios since the biogas available is considered as stable. The cost function for the
 426 anaerobic digestion section has been retrieved from (Mehr et al., 2017), where it was
 427 discussed in detail. The cost was scaled down, starting from a literature source, with
 428 an exponential factor of 0.75.
- 429 - The costs of the cleaning system, again constant for the 4 scenarios, which was used
 430 in both (Mehr et al., 2017; MosayebNezhad et al., 2018) and was derived from a

431 dedicated workshop on cleaning systems for fuel cell applications (Argonne National
432 Laboratory et al., 2014). The cost will be analyzed in a current/short-term scenario
433 (500 \$/kWe) and in a long-term scenario (200 \$/kWe).

434 - The cost of the three SOFC modules, constant in all the scenarios, derived from the
435 Roland Berger's Consultancy report for the FHC-JU funding agency (Roland Berger
436 Strategy Consultants, 2015). As for the cleaning system, because of the innovative
437 nature of the technology, a short-term cost (equal to 5,656 €/kWe) and a long-term
438 cost (equal to 2,326 €/kWe) have been analyzed. Both the data are derived from the
439 reference document and referred to different cost production volumes, as discussed in
440 detail in (MosayebNezhad et al., 2018). Current costs from the mentioned reference
441 (17,908 €/kW) are not analyzed since, as shown in the authors' previous works, no
442 economic convenience is achievable with these cost levels. Short term costs can be
443 considered as 'future' cost due to an increase of production volumes or current costs
444 with an incentive on the investment, supplied by local governments (as happens in the
445 U.S.) or by dedicated projects.

446 - The cost of the Heat Recovery Unit, which has been assumed constant and equal to
447 the one designed in (MosayebNezhad et al., 2018).

448 - The cost of the solar system for scenario B, taken from (Cavalcanti and Motta, 2015;
449 Mehr et al., 2017) and equal to 2710 \$/m² (with a reference solar collector area of 500
450 m²).

451 - The cost of the MGT for scenario C, taken from (MosayebNezhad et al., 2018; Pierce,
452 2005) and equal to 1,000 €/kWe.

453 - The cost of the Trigeneration section for the scenario D, which includes the cost of the
454 TLC system (taken from (Fischer, 2011; Mehr et al., 2018; Yari et al., 2015) and
455 expressed as a function of the expander power) and the cost of the chiller unit
456 (expressed as a function of the cooling power produced and retrieved from (Berliner
457 Energieagentur GmbH (Project coordinator), 2009)).

458 For what concerning the Operating Expenditure, they have been evaluated as the sum of:

459 - Cleaning system operating costs, due to the cleaning sorbents yearly substitution,
460 taken from (Argonne National Laboratory et al., 2014) and equal to 1 c\$/kWh in the
461 short-term scenario and 0.5 c\$/kWh in the long-term scenario.

- 462 - SOFC modules general yearly maintenance, retrieved from (Roland Berger Strategy
463 Consultants, 2015) and equal to a fixed value of 3,000 € in the short-term scenario
464 and 2,350€ in the long-term scenario.
- 465 - SOFC stack substitution, occurring every 5 years in the short-term scenario (with a
466 cost equal to 712 €/kWe) and every 7 years in the long-term scenario (with a cost
467 equal to 482 €/kWe) (Roland Berger Strategy Consultants, 2015).
- 468 - Anaerobic Digester maintenance and Solar Collectors maintenance, expressed as 5 %
469 of the relative CAPEX (Mehr et al., 2017), while Trigeneration section maintenance
470 expressed as 4 % of the CAPEX.
- 471 - MGT section maintenance, equal to 1 c€/kWh from (MosayebNezhad et al., 2018).
- 472 - Cost of NG from the grid, when heat produced from the plant is not enough to supply
473 the plant thermal load (digester heating). The price of energy streams (electricity and
474 heat) has been first set as the one in the SMAT Collegno case study and then varied to
475 analyze possible installation throughout all the EU area.

476 The third cost item which is included in the analysis is the quota related to the savings, which
477 in the 4 analyzed scenarios are accounting for:

- 478 - Savings for electricity, equal (in all Scenarios) to the total yearly electrical production
479 (kWh), available from the energy model, multiplied by the price of electricity
480 (€/kWh).
- 481 - Savings for heating, accounted (in Scenario 2, 3 and 4) as natural gas saved for
482 producing the same amount of thermal power. The calculation has been performed
483 with a boiler efficiency of 95 % and a NG LHV of 47 MJ/kg.
- 484 - Savings for cooling accounted (in Scenario 4) as electricity saved for the production
485 of the same amount of cooling thermal power. The calculation was performed with a
486 Coefficient of Performance (COP) equal to 3.5.

487 All the analysis is based on the assumption the WWTP is self-consuming all the energy
488 produced (electricity, heating and cooling) because, as deeply discussed in one of the authors'
489 previous work (Gandiglio et al., 2017), WWTPs are energy intensive plants which require a
490 high amount of energy to reach their goal (clean the inlet wastewater). Furthermore,
491 especially for the Italian case, self-consumption is also the most convenient choice because
492 there is no incentive available for electricity sold to the grid which would be paid in a range
493 between 0.04 and 0.06 €/kWh (strongly lower than the price paid for electricity).

494 2.6.2 Baseline case study analysis

495 The first baseline analysis has been performed with energy price related to the SMAT
496 Collegno case study, which is equal to 0.141 €/kWh and 0.526 €/Sm³, available as average
497 2017-2018 values for the site (“SMAT, Società Metropolitana Acque Torino S.p.A., Turin,
498 IT.,” 2019). A summary of the CAPEX, OPEX and savings values for the four different
499 scenarios in short-term view with baseline energy cost is available in Appendix A.

500 Starting from the input data discussed above, a complete cash flow analysis has been
501 performed for the baseline case study (the Collegno WWTP), following the methodology
502 discussed in (Mehr et al., 2017; MosayebNezhad et al., 2018) with an interest rate of 5 % and
503 performing the analysis on a system lifetime of 15 years.

504 Pay Back Time (PBT) – expressed as the first year in which the cash flow turns to positive –
505 has been used as a first economic performance indicator, and has been calculated as:

$$PBT(y) = (1 + n_y - n/p) \quad (40)$$

506 Where:

- 507 - n_y is the number of years after the initial investment at which the last negative value
508 of cumulative cashflow occurs.
- 509 - n is the value of cumulative cashflow at which the last negative value occurs.
- 510 - p is the value of the present cashflow at which the first positive value of cumulative
511 cash flow occurs.

512 The second economic indicator used is the Levelized Cost of Electricity, which has been
513 calculated as:

$$LCOE \left(\frac{\text{€}}{\text{kWh}} \right) = \frac{\sum_{t=1}^n \frac{CAPEX_t + OPEX_t}{(1+r)^t}}{\sum_{t=1}^n \frac{E_t}{(1+r)^t}} \quad (41)$$

514 Where:

- 515 - $CAPEX_t$ is the investment cost in year t
- 516 - $OPEX_t$ is the operating and maintenance cost in year t
- 517 - E_t is the electricity generation in year t
- 518 - r is the discount rate

519 - n is the lifetime of the system.

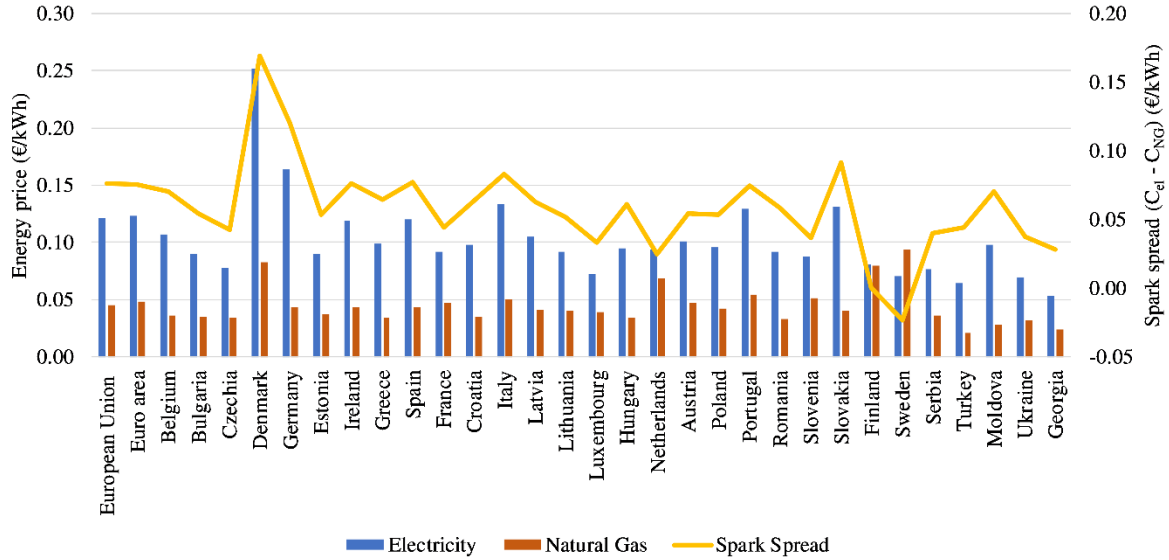
520 **2.6.3 EU area economic analysis**

521 The second phase of the economic evaluation has been the analysis of the investment
522 considering different EU countries and thus different energy and NG prices. The energy
523 prices for the different countries analyzed are referred to the second semester of 2018 and
524 have been taken from the Eurostat online database for electricity (Eurostat - Data Explorer,
525 2019a) and NG (Eurostat - Data Explorer, 2019b) for non-household (industrial) consumers
526 (take as full price, ‘including all taxes and levels’). Since the energy price is varying with the
527 annual energy consumption according to defined ranges, yearly data have been derived from
528 the baseline scenario. The electrical yearly consumption of the overall WWTP has been
529 assumed equal to the one of SMAT Collegno (~ 5,500 MWh/y) and the related range of
530 2,000-20,000 MWh/y has been selected. The range allows also for a variation in the real plant
531 consumption without varying the energy prices. The NG yearly consumption has been indeed
532 taken from the energy model, because the thermal balance of the anaerobic digester (which is
533 usually the highest and most relevant NG consumption within the WWTP) was included in
534 the model. According to the different scenarios, yearly NG consumption was varying
535 between ~ 2,100 and 3,300 GJ/y and so the Eurostat range between 1,000 and 10,000 GJ/y
536 has been chosen.

537 Starting for these data, and focusing especially on the spark spread, defined as the difference
538 between the national electricity price (c_{El}) and the NG price (c_{NG}):

$$Spark\ Spread = c_{El}(\text{€/kWh}) - c_{NG}(\text{€/kWh}) \quad (42)$$

539 A summary of energy prices is available in Figure 6.



541

542 Figure 6. Price of electricity and natural gas in different EU countries. Authors' own elaboration of data from
543 (Eurostat - Data Explorer, 2019a, 2019b).

544 In order to analyze all the countries included in the EU area with a simple approach, a new
545 definition of the economic performance evaluators has been also formulated. The interest rate
546 effect has been neglected since the goal is to analyze the relative difference among the
547 different countries. Furthermore, in the baseline scenario analysis, it has been evaluated that
548 the effect of the interest rate (set as 5 %) is varying between 12 % and 26 % depending on the
549 analyzed scenario; this information is useful to understand the possible error undergone when
550 using the simplified equations. Simplified Pay Back Time (S_PBT) and Simplified Levelized
551 Cost Of Electricity (S_LCOE) have been expressed as follows.

$$S_PBT(y) = \frac{CAPEX(\text{€})}{Net\ yearly\ savings(\text{€}/y)} = \frac{CAPEX(\text{€})}{Savings - OPEX(\text{€}/y)} \quad (43)$$

$$S_LCOE(\text{€}/kWh) = \frac{CAPEX(\text{€}) + OPEX_{tot}(\text{€})}{Total\ electrical\ production(kWh)} = \frac{CAPEX(\text{€}) + OPEX(\text{€}/y) \cdot N(y)}{Yearly\ production(kWh) \cdot N(y)} \quad (44)$$

552 3. Results and discussion

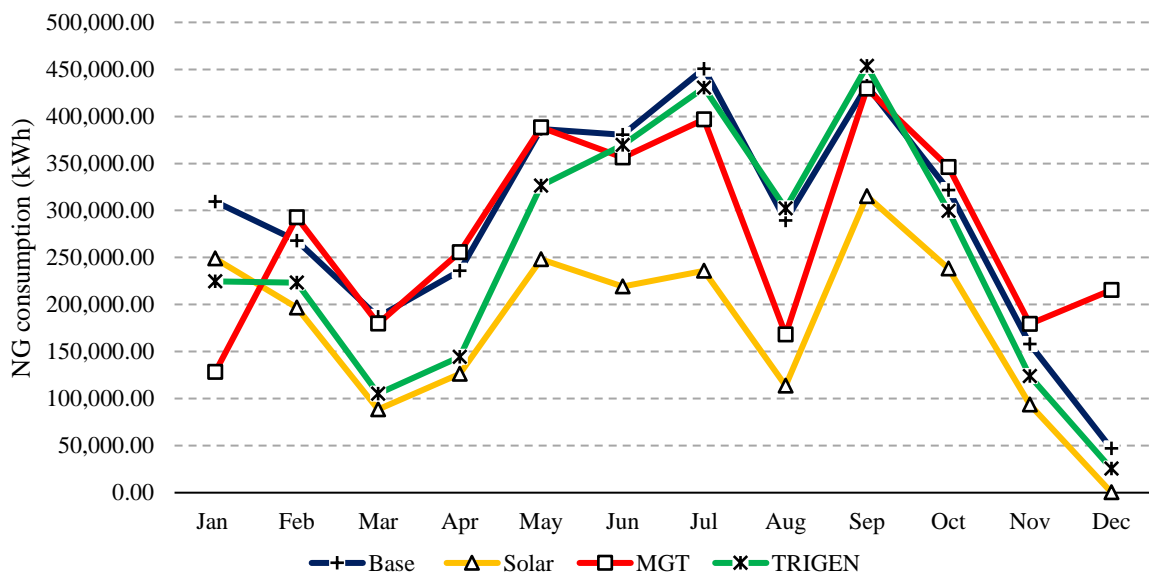
553 In this section results of the energy simulations and techno-economic analysis are presented
554 and deliberated.

555 3.1 Energy simulation results

556 To supply the thermal demand for the plant, NG consumption (kWh) is obtained for each
557 scenario. The results are demonstrated in Figure 7. The NG supplied to the systems from the

558 grid is the most for the base case scenario as the system has to produce the thermal energy on
 559 its own. The second most case is the MGT case in which the MGT requires an extra amount
 560 of NG to produce extra electrical power. The solar case is the optimum scenario from the NG
 561 consumption point of view. In this case, the amount of NG would be reduced by about 50 %
 562 on average. In addition, the trend of the NG required in the plant is similar for the studied
 563 case. It indicates that during the summer season as the biogas produced in the plant is the
 564 lowest, the amount of NG requirement would increase in order to compensate for the
 565 reduction in the amount of biogas. For the trigeneration case, it can be observed that during
 566 winter and fall, the NG consumption is low similar the solar case, however, during summer
 567 when the biogas production is low, NG consumption of the trigeneration case reaches to the
 568 values for the base case, even higher than that of the MGT case.

569

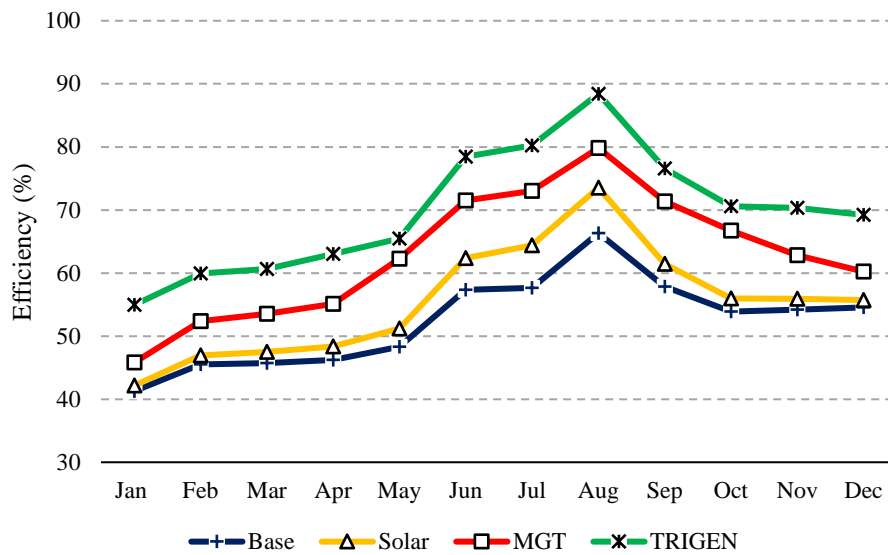


570

571

Figure 7. Monthly natural gas consumption for all case studies.

572 Results of efficiency for the proposed systems are illustrated in Figure 8. As the figure
 573 indicates, the overall efficiency for the trigeneration system is the highest while the base case
 574 has the lowest efficiency. The maximum efficiency of the trigeneration system can reach 89
 575 % in August. The second most effective is related to the case of MGT in which extra power
 576 can be produced by means of micro gas turbines. It is also shown that the solar case
 577 efficiency was not so much different from that of the base case except for some months
 578 during the summer when the solar thermal energy utilization would be efficiently done.



579

580

Figure 8. Monthly energy efficiency analysis for the defined case studies.

581

The total electrical power produced by the proposed systems is shown in Figure 9. Referring to this figure, the highest amount of electrical power is produced by the MGT case in which microturbines have the responsibility to produce extra power. For the trigeneration case, extra power would be produced by means of the expander while it is not comparable with that of the MGT case. It can be observed that about 275 kW could be produced in MGT case while in trigeneration case approximately 200 kW could be produced. One important point is that during summer season the MGT system would operate in partial load, as there is not so much need to produce extra thermal energy for the digester. As a result, the produced power via MGT would decrease and consequently, the overall electrical power would become lowest during summer. Electrical power in Solar and base is identical as there is no an additional source of power production. The sole power production system is the SOFC units themselves.

582

583

584

585

586

587

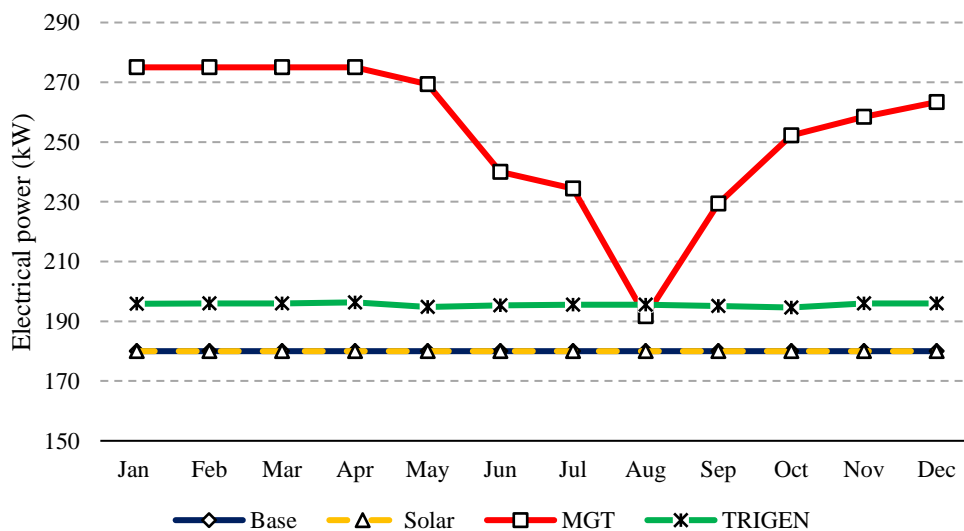
588

589

590

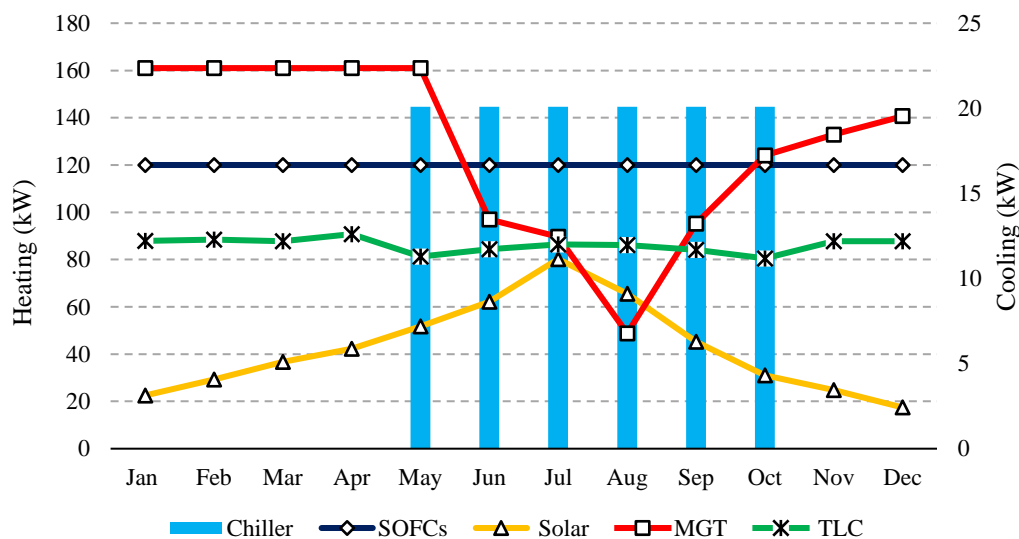
591

592



593

595 In Figure 10 heating and cooling contributions of each auxiliary system are illustrated.
 596 Referring to this figure, as the base case is selected as the reference case, there is not any
 597 additional equipment in providing heating and cooling so SOFC exhaust gases and the boiler
 598 would provide the heating. However, for the solar case, solar collector can provide 20kW to
 599 70kW heating depends on the time position. Clearly, during summer solar system could
 600 provide the most possible thermal energy rather than other seasons. In the case of a
 601 trigeneration system, uniform heating amount of about 90 kW could be produced. In addition,
 602 by implementing a trigeneration system, during summer about 22 kW cooling can be utilized.
 603 For MGT case, heating power produced by microturbines strongly depends on the heat load
 604 requirement of the whole plant. As it can be observed, during summer when SOFC and boiler
 605 can supply the demand, there would be not extreme need for other equipment so that
 606 microturbines would not run in full load, and as the trend shows during this period the
 607 heating by the MGT is lower.



608

609 Figure 10. Heating and cooling rates produced by the different units in the proposed scenarios.

610 **3.2. Techno-economic findings**

611 Results of the performed techno-economic analysis are presented as follows.

612 **3.2.1 Baseline case study results**

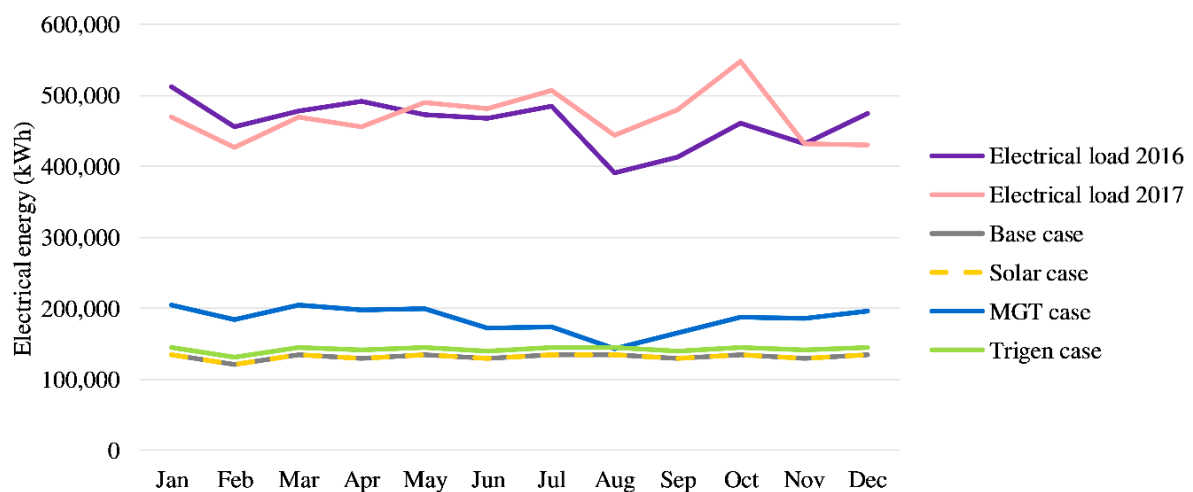
613 This section is devoted to the analysis of the techno-economic model results. From the energy
 614 model, monthly electrical load profiles are available, and these data have been compared with
 615 SMAT Collegno electrical load of years 2016 and 2017 (Figure 11). The yearly coverage in
 616 the four scenarios (with 2017 data) is respectively 28 % for the Base and Solar Cases, 39.4 %

617 for the MGT case and 30.4 % for the Trigen Case. The use of the hybrid SOFC-MGT system
 618 is generating an increase in the electrical coverage of more than 10 %, and this will also
 619 affect positively the economic performance, as will be shown in the next paragraph. The
 620 Trigen Case increase is relatively low (around 2 %); however, extra-heat and extra-cooling
 621 are also available, and this will be accounted for in the economic analysis. Anyway,
 622 electricity is the key product for the plant and generates the highest saving (in €/kWh).

623 By using the economic model and input data described in section 2.6, investment (CAPEX),
 624 operating costs (OPEX) and savings for the four scenarios have been calculated. Results are
 625 shown in Figure 12, Figure 13 and Figure 14 for the Short-Term Cost scenario (which is
 626 related to cleaning unit investment and operative costs, SOFC modules investment, operation
 627 and lifetime).

628 Figure 12 shows the share of CAPEX items for the 4 different scenarios, for the Short-Term
 629 cost scenario. The SOFC module (5,656 €/kWe) is the highest share of investment in all the
 630 case studies (between 77 % and 85 % of total plant cost), followed by the cleaning unit (~ 6.5
 631 %) and the anaerobic digestion section (~ 7 %). The MGT equipment (7.3 %), when present,
 632 is also comparable with cleaning unit and AD cost. Effect of the trigeneration section is
 633 indeed less impacting (5.2 %), while solar collectors account for around 9 %. On absolute
 634 values, as expected, higher costs are related to the three modified scenarios respect to the
 635 Base Case and the highest cost is related to the Solar Case where the investment cost of
 636 hybridization plays a decisive role. The costs share is, of course, changing when moving to
 637 the Long-Term Costs scenario, where SOFC share of the total cost is between 62 and 75 %.

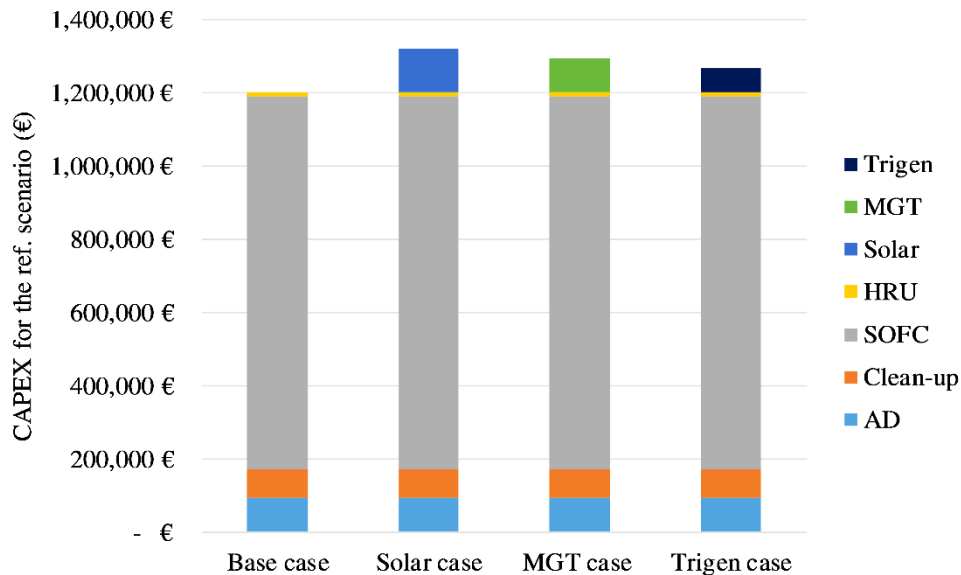
638



639

640

Figure 11. Electrical load coverage in the different analyzed scenarios.



641

642

Figure 12. Investment cost (CAPEX) for the four analyzed scenarios.

643

644

645

646

647

648

649

650

651

652

653

654

655

656

657

658

Concerning the operating costs over the lifetime (OPEX), results for the Short-Term Cost Scenario are shown in Figure 13. In WWTPs, where the inlet biomass solid content is relatively low (~2 %), the need for thermal energy to reach the digester operating temperature is high compared to other biogas plants (based on agricultural or organic waste biomass) and this generates the need of extra-NG to be fed to the boiler for supplying the overall yearly thermal request (extra respect the CHP production). Furthermore, NG can be used to keep the CHP operation constant during the year, when biogas is reduced (see energy model chapter for further details). The NG bought from the grid is, as shown in Figure 13, the higher share in OPEX of the biogas section of the WWTP, followed by the stack substitution and the general maintenance of the plant BoP (called ‘other maintenance’ in the figure), the stack substitution (taken from (Roland Berger Strategy Consultants, 2015)) and the cleaning unit maintenance. The other OPEX items are almost negligible compared to the total cost volume (which is in the range of 100-130 k€/y). Among the four cases, Solar case results in the lowest OPEX because the total NG consumption is lower. OPEX costs are affected by the Long-Term Cost Scenario only for what concerns the OPEX of biogas clean-up and SOFC maintenance, while all the other cost items (like NG) remain constant.

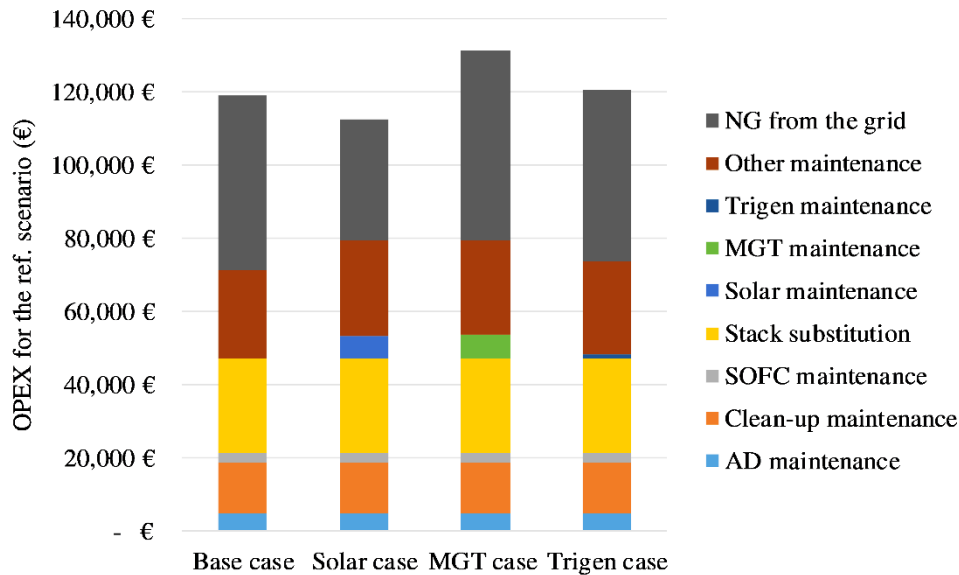
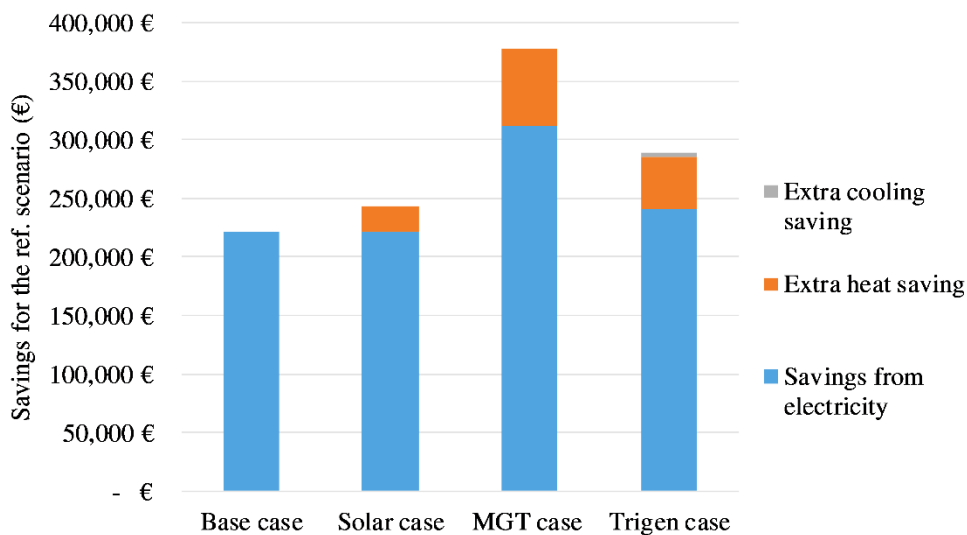


Figure 13. Operative cost (OPEX) for the four analyzed scenarios.

659

660

661 The amount of savings generated from the operation of the plant under the baseline scenario
 662 is shown in Figure 14. As previously commented, the highest share of saving is given by
 663 electricity self-consumption because this is the stream resulting in the highest monetary
 664 value. This amount is constant among Base and Solar Case while strongly increases in the
 665 hybrid MGT case. Trigen Case is an intermediate situation among the previous ones. Heating
 666 and cooling savings are also accounted for as discussed in the methodology section.



667

668

Figure 14. Savings (from electricity, heating and cooling) for the four analyzed scenarios.

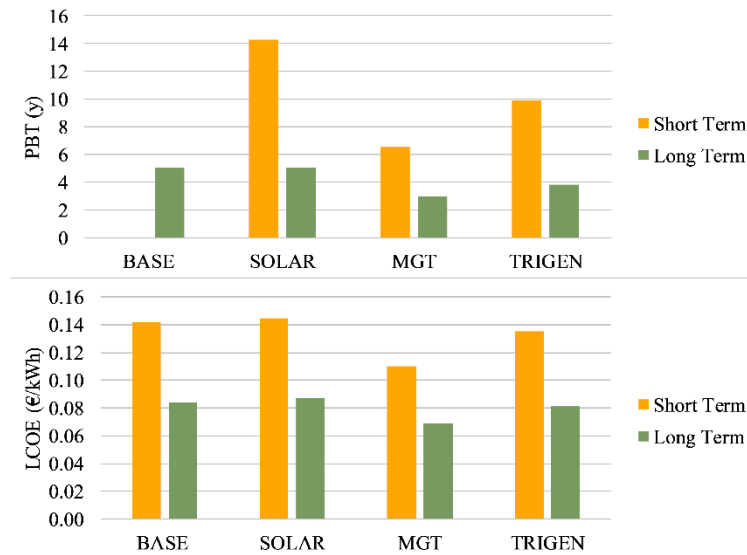


Figure 15. Short and Long term cost scenarios comparison. Effect on PBT and LCOE.

669

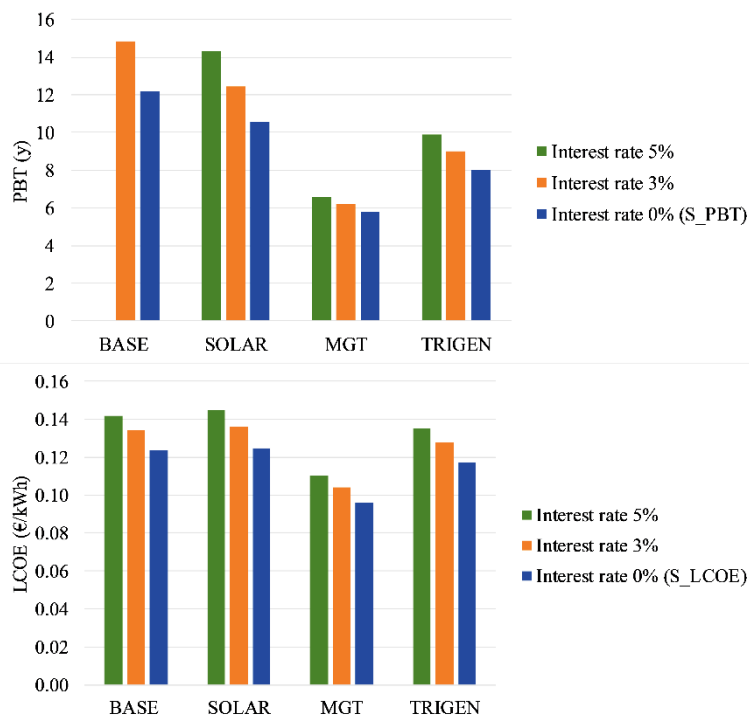
670

671 Economic performance indicators (PBT and LCOE) are then calculated, for the Baseline
 672 Scenario, starting from the presented data. Results for both Short-Term and Long-Term Cost
 673 Scenarios and for 4 Cases are presented in Figure 15. As a general instruction to the
 674 following graphs, when PBT is not plotted is because it is higher than the plant lifetime
 675 (assumed as 15 years). This situation is happening, for example, in the Base Case Short-Term
 676 case study, where also LCOE is very high, equal to 0.1418 €/kWh, higher than electricity
 677 price. The other case studies (Solar, MGT and Trigen) are – even if with long PBT – able to
 678 generate an investment recovery during the plant lifetime. Among the three cases, MGT Case
 679 is the one showing the lowest PBT (6.58 y in Short-Term) and LCOE (0.1100 €/kWh),
 680 followed by the Trigen and the Solar Case. Moving from Short- to Long-Term Costs, a
 681 general benefit can be seen in the whole analysis. Having lower investment and operating
 682 costs generate a positive effect on the analysis and almost all the cases become interesting
 683 from an economic point of view, with PBT ranging from 2.95 (MGT) to 5.03 (Solar) and
 684 LCOE between 0.0688 (MGT) and 0.0866 (Solar) €/kWh. The reason for having a switch on
 685 the worst case between Short-Term and Long-Term cost scenarios is the share of the solar
 686 collectors in the overall plant CAPEX. In the Short-Term case, solar influence is low and
 687 higher electrical production produces more benefits than Base Case in terms of economics
 688 while moving to the Long-Term, the effect of solar collectors on CAPEX share is heavier and
 689 this results in a decrease of the economic evaluator.

690 The Long-Term scenarios seem indeed to be economically acceptable without the help of any
 691 external subsidy, while the Short-Term is feasible for some configurations only (MGT) and
 692 remains quite challenging for the Base Case. An existing Ministerial Decree on electricity
 693 production from biogas is existing (Ministero dello Sviluppo Economico, 2016). However,

694 the price paid for the electricity from sewage WWTP biogas (11 c€/kWh) is lower than the
 695 price paid by SMAT (14.1 €/kWh) and thus the most economic use of the electricity is self-
 696 consumption.

697



698

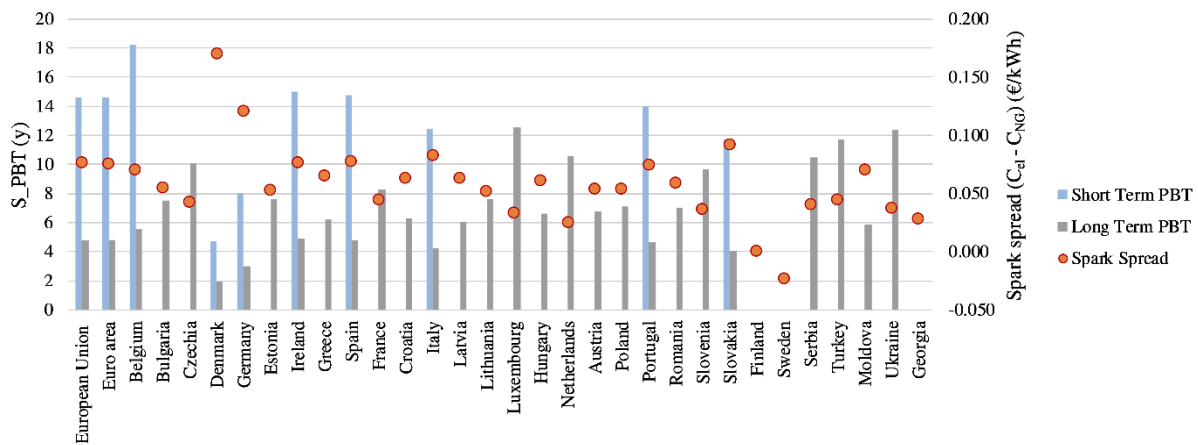
699 Figure 16. Interest rate effect (0 %-3 %-5 %) on PBT and LCOE. Interest rate equal to 0 % is the same as the
 700 simplified values.

701 The second analysis performed on the Baseline Scenario is on the effect of the interest rate on
 702 the economic performance evaluators. The results are then useful to understand the values of
 703 the next EU Scenario, where the interest rate was fixed to zero in order to analyze a more
 704 simplified scenario. As shown in Figure 16, the effect of the interest rate effect is low. When
 705 moving from an interest rate of 5 % to 0 % (simplified scenario), the PBT is reduced by 12-
 706 26 % in all the four Cases and LCOE by 13-14 %. A lower impact of the interest rate can be
 707 found on the LCOE, and this is motivated by the different formulations of the two
 708 parameters.

709 3.2.2 EU area: results from the economic analysis

710 Starting from the Baseline SMAT Collegno analysis, the model has then been extended to the
 711 whole EU area, taking advantage of available energy prices from the Eurostat database, as
 712 discussed in section 2.6.

713 Results are shown in Figure 17 and they refer to the Base Case Scenario (only biogas and
 714 SOFC, without hybridization). The graph shows the direct correlation between investment
 715 performance and the difference between electricity and NG price for each country (i.e., the
 716 spark spread). This is even more visible in extreme situations like those in Finland and
 717 Sweden, where the spark spread is very low and the S_PBT is thus never reached during the
 718 plant lifetime. Otherwise, for countries like Denmark, Germany and Italy – where the spread
 719 is higher, the investment is profitable, even with Short-Term costs.

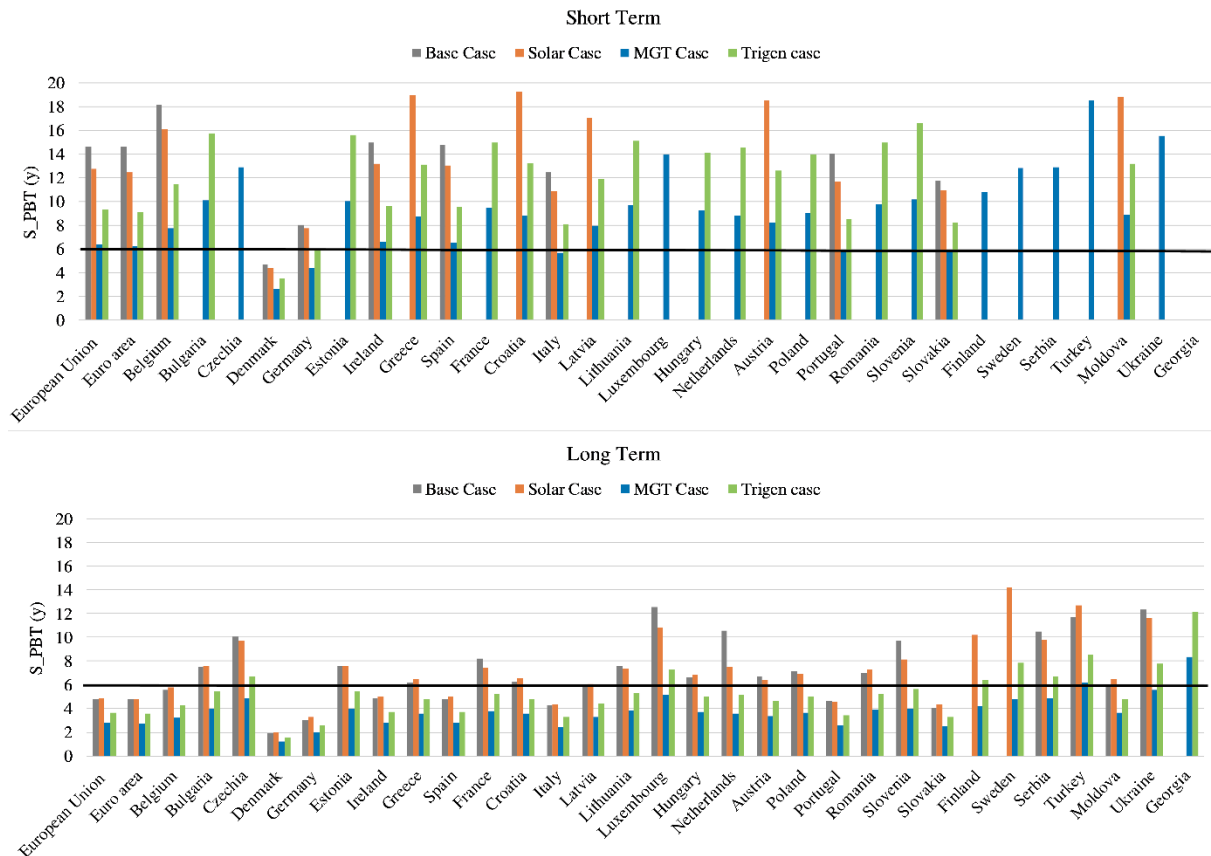


720 Figure 17. EU analysis: Base Case results and correlation among S_PBT and spark spread values. Light blue
 721 bars refer to the Short-Term costs, light grey bars to the Long-Term costs and orange points to the spark spread
 722 in each country.
 723

724 The relation between the economic performance and both electricity and NG prices is due to
 725 the need, in many WWTPs, of both electricity and NG to supply the required thermal load. In
 726 the case of optimized plants with reduced, or even zero, thermal load (achievable for example
 727 with the use of a sludge pre-thickening system as demonstrated in Ref. (Giarola et al., 2018)),
 728 the economic performance will depend only on the electricity price and results will vary
 729 consequently.

730 It is important to remind that all the EU analysis is based on simplified economic parameters
 731 (S_PBT and S_LCOE) and thus results are generally underestimated (real values with interest
 732 rate would be around 15-20 % higher, according to the results shown in 3.2.1).

733 Moving from the Base Case Scenario to the whole 4 scenarios analysis, Figure 18 and Figure
 734 19 show S_PBT and S_LCOE with Short- and Long-Term costs for the different EU
 735 countries. For the S_PBT, a target value of 6 years is set as a goal (black line in Figure 18),
 736 while for the S_LCOE the values are plotted against the price of electricity; when electricity
 737 price is higher than production cost (S_LCOE), the investment is convenient and there is a
 738 net saving between production and self-consumption.



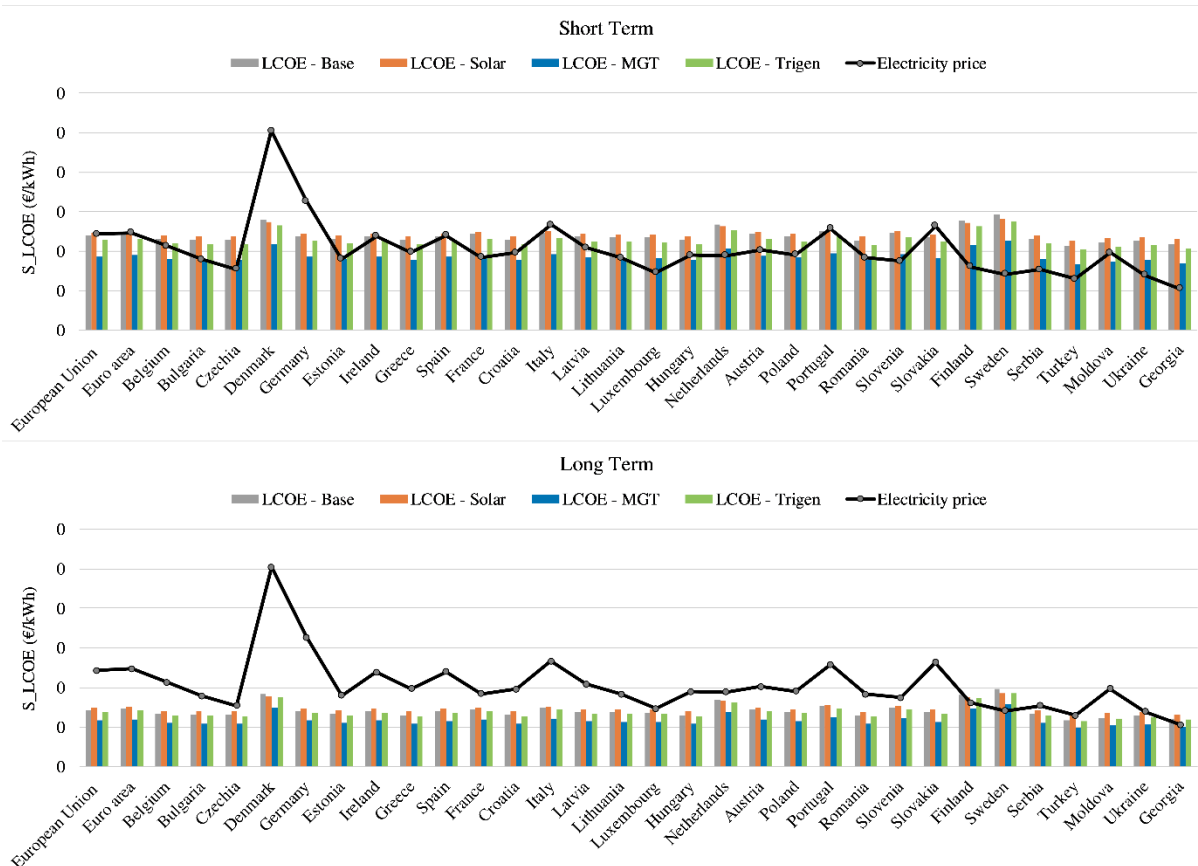
739

740

Figure 18. EU analysis: Short and Long term scenarios effect on PBT for the four scenarios.

741 In Figure 18, in the Short-Term Costs analysis, countries with PBT lower than or equal to 6
 742 years, in one of the 4 cases, are only Denmark (in all cases), Germany, Italy, Portugal and
 743 Slovakia (only in MGT case). The other countries show higher S_PBT, which are usually
 744 closer to the plant lifetime (15 years), which is not acceptable from an economic point of
 745 view. Looking at the Long-Term cost analysis, all the countries become economically
 746 interesting ($S_PBT < 6$ years) in at least the MGT case but usually also in the other proposed
 747 configurations.

748 The Long-Term scenario could be considered as a future scenario where the cost of the
 749 technology will be reduced (thanks to the mass production), or a current scenario where an
 750 incentive on the investment is given for high efficiency and zero emissions fuel cell systems.
 751 In both cases, biogas-fed SOFC systems will become economically interesting and
 752 comparable with traditional technologies.



753

754

Figure 19. EU analysis: Short and Long term effect on LCOE (vs. country electricity price).

755 The same concept can be observed for what concerning the S_LCOE: the Short-Term cost
 756 analysis (upper graph of Figure 19) is showing a not-too-bad and not-too-good scenario,
 757 where the production cost (S_LCOE) is comparable with the country electricity price: this is
 758 the reason why, as confirmed by the previous figure, the PBT is comparable with the plant
 759 lifetime. On the other side, moving to the Long-Term cost analysis, as already demonstrated
 760 in the S_PBT analysis, the production price (S_LCOE) is always (except in specific countries
 761 like Finland and Sweden) higher than the electricity price, and this is generating a net income
 762 for every kWh produced.

763 Finally, the economic analysis has pointed out the countries and the areas where the biogas-
 764 fed SOFC system could generate the highest financial benefits because of the positive energy
 765 price conditions and these are Germany, Denmark, Slovakia, and Italy (in the current cost
 766 scenario without incentives). In the case of a further reduction in SOFC manufacturing cost
 767 (because of production volume, technology learning, and dedicated incentives,) almost all the
 768 EU area will become an interesting market for the SOFC modules. The most critical
 769 countries, on the other side, have been identified as Sweden and Finland.

770 4. Conclusions

771 There is the potential to use the thermal energy from the exhaust gas of a biogas-fed SOFC
772 system to meet a part of the energy demand of wastewater treatment plants. Four scenarios
773 are investigated by looking at the integration of solar collectors, microturbines, trilateral
774 Rankin cycle, and absorption chiller with the SOFC in order to increase the overall plant
775 efficiency. Along with supplying the electrical demand of the plant and thermal demand of
776 the digester, a focus on the reduction of natural gas consumption for the proposed systems is
777 performed. In addition, a comprehensive techno-economic investigation is performed. The
778 following conclusions can be drawn from the results:

- 779 • The trigeneration system attains the highest thermal efficiency among the proposed
780 scenarios.
- 781 • The natural gas consumption is comparatively low for the solar integrated system
- 782 • The electrical demand supplied by the MGT case is promising
- 783 • MGT Case is also effective from the economic point of view since it is found to be
784 the most interesting case in terms of PBT and LCOE compared to other system
785 configurations.
- 786 • Hybridization of the system with solar collectors or trigeneration could play a
787 fundamental role for the end-user self-sufficiency rate and from the environmental
788 point of view but is not currently suggested from the economic point of view since the
789 investment cost is increased in a comparable way to the savings and thus the
790 economic evaluators are almost constant.
- 791 • SOFC short and long term cost trajectories suggested by EU funded studies (Roland
792 Berger Strategy Consultants, 2015) have a huge impact on the economic performance.
793 If, thanks to dedicated incentives on the investment or to mass production volumes,
794 SOFC CAPEX would decrease at around 2,300 €/kW, the economic competitiveness
795 of biogas-fed SOFC systems, in different hybrid configurations, would be reached in
796 most of the EU countries. Short term cost reduction, leading to an investment cost of
797 around 5,600 €/kW, would generate anyway interesting niche markets in specific EU
798 countries where the energy prices are favorable for CHP installations.
- 799 • The analysis of the whole EU area has indeed pointed out a direct and proportional
800 link between the spark spread in the selected country and the economic performance
801 of the investment. The more the electricity is expensive compared to the NG, the more

802 a high-efficiency cogeneration system is interesting for an industrial plant. In this
803 scenario, most favorable markets for SOFC installation – in a short-term view – are
804 Germany, Denmark, Slovakia, and Italy. The area could also be enlarged is long term
805 cost trajectories will be reached or specific incentives on investment (for high-
806 efficiency CHP system) will be issued.

807 **5. Acknowledgments**

808 SMAT S.p.A. is acknowledged for sharing valuable data on the operation of Collegno
809 WWTP. The research of the corresponding author is supported by a grant from University of
810 Bonab (Contact number: 97/I/ER/1921).

811 6. References

- 812 Argonne National Laboratory, U.S. Department of Energy, Fuel Cell Technologies Office,
813 2014. Gas Clean-Up for Fuel Cell Applications Workshop - March 6-7, 2014.
- 814 Basrawi, F., Ibrahim, T.K., Habib, K., Yamada, T., Daing Idris, D.M.N., 2017. Techno-
815 economic performance of biogas-fueled micro gas turbine cogeneration systems in
816 sewage treatment plants: Effect of prime mover generation capacity. *Energy* 124, 238–
817 248.
- 818 Berliner Energieagentur GmbH (Project coordinator), 2009. SUMMERHEAT: Meeting
819 cooling demands in SUMMER by applying HEAT from cogeneration.
- 820 Bicer, Y., Dincer, I., 2015. Energy and exergy analyses of an integrated underground coal
821 gasification with SOFC fuel cell system for multigeneration including hydrogen
822 production. *Int. J. Hydrogen Energy* 40, 13323–13337.
- 823 Capstone Microturbine Products, 2017. URL www.capstoneturbine.com/ (accessed 9.9.17).
- 824 Cavalcanti, E.J.C., Motta, H.P., 2015. Exergoeconomic analysis of a solar-powered/fuel
825 assisted Rankine cycle for power generation. *Energy* 88, 555–562.
- 826 Cheddie, D.F., Murray, R., 2010a. Thermo-economic modeling of a solid oxide fuel cell/gas
827 turbine power plant with semi-direct coupling and anode recycling. *Int. J. Hydrogen*
828 *Energy* 35, 11208–11215.
- 829 Cheddie, D.F., Murray, R., 2010b. Thermo-economic modeling of an indirectly coupled solid
830 oxide fuel cell/gas turbine hybrid power plant. *J. Power Sources* 195, 8134–8140.
- 831 Cui, S.-H., Li, J.-H., Jayakumar, A., Luo, J.-L., Chuang, K.T., Hill, J.M., Qiao, L.-J., 2014.
832 Effects of H₂S and H₂O on carbon deposition over La_{0.4}Sr_{0.5}Ba_{0.1}TiO₃/YSZ perovskite
833 anodes in methane fueled SOFCs. *J. Power Sources* 250, 134–142.
- 834 DEMOSOFC project official website, 2018. URL www.demosofc.eu (accessed 2.20.18).
- 835 Eurostat - Data Explorer, 2019a. Electricity prices for non-household consumers - bi-annual
836 data (from 2007 onwards)
- 837 Eurostat - Data Explorer, 2019b. Gas prices for non-household consumers - bi-annual data
838 (from 2007 onwards) [WWW Document].
- 839 Eveloy, V., Karunkeyoon, W., Rodgers, P., Al Alili, A., 2016. Energy, exergy and economic
840 analysis of an integrated solid oxide fuel cell – gas turbine – organic Rankine power
841 generation system. *Int. J. Hydrogen Energy* 41, 1–16.
- 842 Firdaus, M., Basrawi, B., Yamada, T., Nakanishi, K., Katsumata, H., 2012. Analysis of the
843 performances of biogas-fuelled micro gas turbine cogeneration systems (MGT-CGSs)
844 in middle- and small-scale sewage treatment plants : Comparison of performances and
845 optimization of MGTs with various electrical power outputs. *Energy* 38, 291–304.
- 846 Fischer, J., 2011. Comparison of trilateral cycles and organic Rankine cycles. *Energy* 36,
847 6208–6219.
- 848 FISIA, 2018. SMAT Collegno WWTP - Anaerobic Digester Sizing report.
- 849 Gandiglio, M., Lanzini, A., Soto, A., Leone, P., Santarelli, M., 2017. Enhancing the Energy
850 Efficiency of Wastewater Treatment Plants through Co-digestion and Fuel Cell Systems.
851 *Front. Environ. Sci.* 5, 70.
- 852 Gandiglio, M., Mehr, A.S., Lanzini, A., Santarelli, M., 2016. DESIGN, ENERGY

853 MODELING AND PERFORMANCE OF AN INTEGRATED INDUSTRIAL SIZE
854 BIOGAS SOFC SYSTEM IN A WASTEWATER TREATMENT PLANT. Proc. ASME
855 2016 14th Int. Conf. Fuel Cell Sci. Eng. Technol. FUELCELL2016 June 26-30, 2016,
856 Charlotte, North Carolina.

857 Giarola, S., Forte, O., Lanzini, A., Gandiglio, M., Santarelli, M., Hawkes, A., 2018. Techno-
858 economic assessment of biogas-fed solid oxide fuel cell combined heat and power
859 system at industrial scale. Appl. Energy 211, 689–704.

860 Guerrini, A., Romano, G., Indipendenza, A., 2017. Energy Efficiency Drivers in Wastewater
861 Treatment Plants : A Double Bootstrap DEA Analysis 1–13.

862 Inui, Y., Matsumae, T., Koga, H., Nishiura, K., 2005. High performance SOFC/GT combined
863 power generation system with CO₂ recovery by oxygen combustion method. Energy
864 Convers. Manag. 46, 1837–1847.

865 Inui, Y., Yanagisawa, S., Ishida, T., 2003. Proposal of high performance SOFC combined
866 power generation system with carbon dioxide recovery. Energy Convers. Manag. 44,
867 597–609.

868 Lackey, J., Champagne, P., Peppley, B., 2017. Use of wastewater treatment plant biogas for
869 the operation of Solid Oxide Fuel Cells (SOFCs). J. Environ. Manage. 203, 753–759.

870 Mazzini, R., 2014. Calore per riscaldamento dalle acque reflue della citta’.

871 Mehr, A.S., Gandiglio, M., MosayebNezhad, M., Lanzini, A., Mahmoudi, S.M., Yari, M.,
872 Santarelli, M., 2017. Solar-assisted integrated biogas solid oxide fuel cell (SOFC)
873 installation in wastewater treatment plant: energy and economic analysis. Appl. Energy
874 191, 620–638.

875 Mehr, A.S., MosayebNezhad, M., Lanzini, A., Yari, M., Mahmoudi, S.M.S., Santarelli, M.,
876 2018. Thermodynamic assessment of a novel SOFC based CCHP system in a
877 wastewater treatment plant. Energy 150, 299–309.

878 Ministero dello Sviluppo Economico, 2016. DECRETO 23 giugno 2016 - Incentivazione
879 dell’energia elettrica prodotta da fonti rin- novabili diverse dal fotovoltaico. Gazz. Uff.
880 DELLA REPUBBLICA ITALIANA. 1–26.

881 MosayebNezhad, M., Mehr, A.S., Gandiglio, M., Lanzini, A., Santarelli, M., 2018. Techno-
882 economic assessment of biogas-fed CHP hybrid systems in a real wastewater treatment
883 plant. Appl. Therm. Eng. 129, 1263–1280.

884 MosayebNezhad, M., Mehr, A.S., Lanzini, A., Misul, D., Santarelli, M., 2019. Technology
885 review and thermodynamic performance study of a biogas-fed micro humid air turbine.
886 Renew. Energy 140, 407–418.

887 National Renewable Energy Laboratory (NREL). System advisor model (SAM)., 2018.

888 Pierce, J., 2005. Capstone 30 kW and 60 kW microturbine installations at landfills, in:
889 Intermountain CHP Application Center Workshop CHP and Bioenergy Bioenergy for
890 Landfills and Wastewater Treatment Plants.

891 Pizza, F., 2015. Welcome to Milano-Nosedo municipal WWTP, The WWTP of Milano
892 Nosedo.

893 Roland Berger Strategy Consultants, 2015. Advancing Europe’s energy systems: Stationary
894 fuel cells in distributed generation. A study for the Fuel Cells and Hydrogen Joint
895 Undertaking.

896 Safari, F., Norouzi, O., Tavasoli, A., 2016. Hydrothermal gasification of Cladophora

- 897 glomerata macroalgae over its hydrochar as a catalyst for hydrogen-rich gas production.
898 *Bioresour. Technol.* 222, 232–241.
- 899 Sánchez, D., Chacartegui, R., Sánchez, T., Martínez, J., Rosa, F., 2008. A comparison
900 between conventional recuperative gas turbine and hybrid solid oxide fuel cell—gas
901 turbine systems with direct/indirect integration. *Proc. Inst. Mech. Eng. Part A J. Power*
902 *Energy* 222, 149–159.
- 903 Santarelli, M., Barra, S., Sagnelli, F., Zitella, P., 2012. Biomass-to-electricity: Analysis and
904 optimization of the complete pathway steam explosion - enzymatic hydrolysis -
905 anaerobic digestion with ICE vs SOFC as biogas users. *Bioresour. Technol.* 123, 430–
906 438.
- 907 SMAT, Società Metropolitana Acque Torino S.p.A., Turin, IT., 2019.
- 908 Sung, T., Kim, S., Kim, K.C., 2017. Thermo-economic analysis of a biogas-fueled micro-gas
909 turbine with a bottoming organic Rankine cycle for a sewage sludge and food waste
910 treatment plant in the Republic of Korea. *Appl. Therm. Eng.* 127, 963–974.
- 911 Wellinger, A., Murphy, J.D., Baxter, D., 2013. *The biogas handbook: science, production and*
912 *applications.* Elsevier.
- 913 Williams, G.J., Siddle, A., Pointon, K., 2001. Design optimisation of a hybrid solid oxide fuel
914 cell and gas turbine power generation system. Harwell Laboratory, Energy Technology
915 Support Unit, Fuel Cells Programme.
- 916 Wongchanapai, S., Iwai, H., Saito, M., Yoshida, H., 2012. Selection of suitable operating
917 conditions for planar anode-supported direct-internal-reforming solid-oxide fuel cell. *J.*
918 *Power Sources* 204, 14–24.
- 919 Xu, L., Dong, F., Zhuang, H., He, W., Ni, M., Feng, S., Lee, P., 2017. Energy upcycle in
920 anaerobic treatment : Ammonium , methane , and carbon dioxide reformation through a
921 hybrid electrodeionization – solid oxide fuel cell system. *Energy Convers. Manag.* 140,
922 157–166.
- 923 Yan, Z., Zhao, P., Wang, J., Dai, Y., 2013. Thermodynamic analysis of an SOFC-GT-ORC
924 integrated power system with liquefied natural gas as heat sink. *Int. J. Hydrogen Energy*
925 38, 3352–3363.
- 926 Yari, M., Mehr, A.S., Mahmoudi, S.M.S., 2013. Simulation study of the combination of
927 absorption refrigeration and ejector-expansion systems. *Renew. Energy* 60, 370–381.
- 928 Yari, M., Mehr, A.S., Mahmoudi, S.M.S., Santarelli, M., 2016. A comparative study of two
929 SOFC based cogeneration systems fed by municipal solid waste by means of either the
930 gasifier or digester. *Energy* 114, 586–602.
- 931 Yari, M., Mehr, A.S., Zare, V., Mahmoudi, S.M.S., Rosen, M.A., 2015. Exergoeconomic
932 comparison of TLC (trilateral Rankine cycle), ORC (organic Rankine cycle) and Kalina
933 cycle using a low grade heat source. *Energy* 83, 712–722.
- 934 Zhang, X., Wang, Y., Liu, T., Chen, J., 2014. Theoretical basis and performance optimization
935 analysis of a solid oxide fuel cell-gas turbine hybrid system with fuel reforming. *Energy*
936 *Convers. Manag.* 86, 1102–1109.
- 937

938 **Appendix A**

939 The tables below summarize the CAPEX, OPEX and savings for the short-term scenario.
 940 Results are here shown for the baseline configuration, with data (energy prices) related to the
 941 SMAT Collegno WWTP.

942 Table A1. CAPEX of the biogas-SOFC plant, in the 4 scenarios.

943

CAPEX (€)								
	AD	Cleaning	SOFC	HRU	Solar	MGT	Trigen	Total CAPEX
Base case	91,816 €	78,945 €	1,018,138 €	10,760 €	- €	- €	- €	1,199,659 €
Solar case	91,816 €	78,945 €	1,018,138 €	10,760 €	118,417 €	- €	- €	1,318,076 €
MGT case	91,816 €	78,945 €	1,018,138 €	10,760 €	- €	95,000 €	- €	1,294,659 €
Trigen case	91,816 €	78,945 €	1,018,138 €	10,760 €	- €	- €	66,491 €	1,266,149 €

944
 945
 946
 947 Table A2. OPEX of the biogas-SOFC plant, in the 4 scenarios.

948

OPEX (€/y)										
	AD maintenance	Cleaning maintenance	SOFC maintenance	Stack substitution	Solar maintenance	MGT maintenance	Trigen maintenance	Other maintenance	NG from the grid	Total OPEX
Base case	4,591 €	13,831 €	3,000 €	25,632 €	- €	- €	- €	23,993 €	47,952 €	118,999 €
Solar case	4,591 €	13,831 €	3,000 €	25,632 €	5,921 €	- €	- €	26,362 €	33,021 €	112,357 €
MGT case	4,591 €	13,831 €	3,000 €	25,632 €	- €	6,402 €	- €	25,893 €	51,845 €	131,194 €
Trigen case	4,591 €	13,831 €	3,000 €	25,632 €	- €	- €	1,169 €	25,323 €	47,067 €	120,613 €

949
 950
 951 Table A3. Savings of the biogas-SOFC plant, in the 4 scenarios.

952

SAVINGS (€/y)				
	Savings from electricity	Extra heat saving	Extra cooling saving	Total savings
Base case	221,604 €	- €	- €	221,604 €
Solar case	221,604 €	21,941 €	- €	243,544 €
MGT case	311,577 €	65,814 €	- €	377,391 €
Trigen case	240,762 €	44,402 €	3,561 €	288,724 €